Conserved residues in yeast initiator tRNA calibrate initiation accuracy by regulating preinitiation complex stability at the start codon

Jinsheng Dong,[1,3] Antonio Munoz,[2,3,4] Sarah E. Kolitz,[2,5] Adesh K. Saini,[1,6] Wen-ling Chiu,[1] Hafsa Rahman,[1] Jon R. Lorsch,[2,4,7] and Alan G. Hinnebusch[1,7]

[1]Laboratory of Gene Regulation and Development, National Institute of Child Health and Human Development, National Institutes of Health, Bethesda, Maryland 20892, USA; [2]Department of Biophysics and Biophysical Chemistry, Johns Hopkins University School of Medicine, Baltimore, Maryland 21205, USA

Eukaryotic initiator tRNA (tRNA$_i$) contains several highly conserved unique sequence features, but their importance in accurate start codon selection was unknown. Here we show that conserved bases throughout tRNA$_i$, from the anticodon stem to acceptor stem, play key roles in ensuring the fidelity of start codon recognition in yeast cells. Substituting the conserved G31:C39 base pair in the anticodon stem with different pairs reduces accuracy (the Sui⁻ [suppressor of initiation codon] phenotype), whereas eliminating base pairing increases accuracy (the Ssu⁻ [suppressor of Sui⁻] phenotype). The latter defect is fully suppressed by a Sui⁻ substitution of T-loop residue A54. These genetic data are paralleled by opposing effects of Sui⁻ and Ssu⁻ substitutions on the stability of methionylated tRNA$_i$ (Met-tRNA$_i$) binding (in the ternary complex [TC] with eIF2-GTP) to reconstituted preinitiation complexes (PICs). Disrupting the C3:G70 base pair in the acceptor stem produces a Sui⁻ phenotype and also reduces the rate of TC binding to 40S subunits in vitro and in vivo. Both defects are suppressed by an Ssu⁻ substitution in eIF1A that stabilizes the open/P$_{OUT}$ conformation of the PIC that exists prior to start codon recognition. Our data indicate that these signature sequences of tRNA$_i$ regulate accuracy by distinct mechanisms, promoting the open/P$_{OUT}$ conformation of the PIC (for C3:G70) or destabilizing the closed/P$_{IN}$ state (for G31:C39 and A54) that is critical for start codon recognition.

[*Keywords*: accuracy; initiation; initiator; scanning; tRNA; translation; yeast]

Supplemental material is available for this article.

Identification of the translation initiation codon in eukaryotic mRNA typically occurs by a scanning mechanism where the 40S ribosomal subunit recruits methionylated initiator tRNA (Met-tRNA$_i$) in a ternary complex (TC) with eIF2-GTP, the resulting 43S preinitiation complex (PIC) attaches to the mRNA 5′ end, and the leader sequence is inspected for complementarity with the anticodon of Met-tRNA$_i$ to identify the AUG start codon (Supplemental Fig. S1; Hinnebusch 2011). The GTP in TC is hydrolyzed in the scanning complex, dependent on eIF5, but P$_i$ release is blocked by eIF1, which also impedes stable binding of Met-tRNA$_i$ in the P site. AUG recognition triggers dissociation of eIF1 from the 40S subunit (Maag et al. 2005), which allows interaction between eIF5 and the C-terminal tail (CTT) of eIF1A (Nanda et al. 2013), P$_i$ release (Algire et al. 2005), and stable binding of TC to the P site (Passmore et al. 2007). Subsequent dissociation of eIF2-GDP and other eIFs enables eIF5B-catalyzed subunit joining and formation of an 80S initiation complex

[3]These authors contributed equally to this work.
Present Addresses: [4]Laboratory on the Mechanism and Regulation of Protein Synthesis, Eunice Kennedy Shriver National Institute of Child Health and Human Development, National Institutes of Health, Bethesda, MD 20892, USA; [5]Immuneering Corporation, One Broadway, 14th floor, Cambridge, MA 02142, USA; [6]Department of Biotechnology, Shoolini University of Biotechnology and Management Sciences, Solan, Himachal Pradesh-173212, India
[7]Corresponding authors
E-mail ahinnebusch@nih.gov
E-mail jon.lorsch@nih.gov
Article is online at http://www.genesdev.org/cgi/doi/10.1101/gad.236547.113.

with Met-tRNA$_i$ base-paired to AUG in the P site (Supplemental Fig. S1; Pestova et al. 2007).

Both eIF1 and scanning enhancer (SE) elements in the eIF1A CTT promote an open, scanning-conducive conformation of the PIC and metastable mode of TC binding (the P$_{OUT}$ state) that allows inspection of P-site triplets during scanning. A scanning inhibitor (SI) element in the eIF1A N-terminal tail (NTT) antagonizes SE function and promotes rearrangement to the closed state (Fekete et al. 2007), with dissociation of eIF1 (Cheung et al. 2007) and more stable binding of TC in the P$_{IN}$ conformation (Supplemental Fig. S2A; Saini et al. 2010). Biochemical mapping experiments for the eIF1A CTT (Yu et al. 2009) and X-ray crystal structures of PICs containing eIF1, eIF1A, or tRNA$_i$ (Rabl et al. 2011; Lomakin and Steitz 2013; Weisser et al. 2013) suggest that the eIF1A CTT and eIF1 physically obstruct Met-tRNA$_i$ binding in the P$_{IN}$ state, thus favoring P$_{OUT}$, whereas the eIF1A NTT likely stabilizes TC binding in the P$_{IN}$ state (Supplemental Fig. S2A).

Genetic experiments have implicated eIF1, eIF1A, eIF5, and eIF2 in accurate AUG selection in living cells. Sui$^-$ (suppressor of initiation codon) mutations in these factors enable initiation at the third, UUG codon in *his4-301* mRNA, lacking the wild-type AUG codon, to restore growth on medium lacking histidine (His$^+$/Sui$^-$ phenotype) (Yoon and Donahue 1992; Donahue 2000; Saini et al. 2010). Most Sui$^-$ mutations in eIF1 weaken its 40S binding and likely enable eIF1 release at near-cognate triplets (Valasek et al. 2004; Cheung et al. 2007; Martin-Marcos et al. 2013). Sui$^-$ mutations in the eIF1A SEs destabilize the open/P$_{OUT}$ conformation, allowing transition from the open/P$_{OUT}$ to closed/P$_{IN}$ state at near-cognates, and also reduce the rate of TC loading (Saini et al. 2010), as TC binds most rapidly to the open conformation (Supplemental Fig. S2B; Passmore et al. 2007). Substitution of residues 17–21 in the eIF1A SI element stabilizes the open/P$_{OUT}$ state, which reduces UUG initiation in Sui$^-$ mutants—the Ssu$^-$ (suppressor of Sui$^-$) phenotype (Fekete et al. 2007)— and also increases the rate of TC binding (Saini et al. 2010) while decreasing the rate of eIF1 dissociation (Supplemental Fig. S2C; Cheung et al. 2007).

tRNA$_i$ contains highly conserved sequences not present in elongator tRNAs (Fig. 1A; RajBhandary and Chow 1995; Marck and Grosjean 2002), with important functions in initiation. The A1:U72 base pair of the acceptor stem enhances eIF2-GTP binding to Met-tRNA$_i$ (Farruggio et al. 1996; Kapp and Lorsch 2004) and TC binding to 40S PICs (Kapp et al. 2006) and is required for wild-type tRNA$_i$ function in yeast cells (von Pawel-Rammingen et al. 1992; Astrom et al. 1993). The three consecutive G:C pairs in the anticodon stem–loop (ASL) promote P-site binding of tRNA$_i$ in eubacteria (Varshney et al. 1993; Mandal et al. 1996). They also confer efficient initiation in mammalian extracts (Drabkin et al. 1993) and enhance the stability of mammalian PICs reconstituted in vitro (Lomakin et al. 2006). In the reconstituted yeast system, the first (G29:C41) and third (G31:C39) of these G:C pairs were found to be required for the stabilizing effect of AUG on the affinity of TC for 43S·mRNA PICs. The deleterious effect on TC binding of substituting

G31:C39 with the corresponding U:U pair in elongator Met-tRNA (tRNA$_e^{Met}$) (Fig. 1A) was mitigated by replacing conserved T-loop residues A54 and A60, suggesting interplay between the T-loop and ASL in AUG recognition by Met-tRNA$_i$ in the P site (Kapp et al. 2006). Surprisingly, however, G31:C39, G29:C41, A54, and A60 were altered to their tRNA$_e^{Met}$ identities without affecting yeast growth (von Pawel-Rammingen et al. 1992), making it unclear whether the function of these residues identified in vitro is important in living cells for the efficiency or accuracy of initiation. To address this last question, we investigated whether substitutions in these and other conserved residues created by site-directed mutagenesis confer Sui$^-$ or Ssu$^-$ phenotypes in yeast cells. We also screened a library of substitutions produced by random mutagenesis for the Sui$^-$ phenotype. Our findings demonstrate that the identities of the third G:C pair of the ASL, T-loop residue A54, and the invariant C3:G70 pair in the acceptor stem are crucial for accurate AUG selection and that these signature residues use distinct molecular mechanisms to discriminate against near-cognate start codons.

Results

Disrupting Watson-Crick pairing at G31:C39 in the ASL increases initiation accuracy

We examined substitutions of tRNA$_i$ for Sui$^-$ or Ssu$^-$ phenotypes using a *his4-301* strain lacking all four genes (*IMT1–IMT4*) encoding the same wild-type tRNA$_i$ and harboring wild-type *IMT4* on a *URA3* plasmid. The latter was replaced with high-copy (hc) *LEU2* plasmids containing the mutant *IMT2* alleles of interest by counterselection with 5-fluoroorotic acid (5-FOA) (Boeke et al. 1987). Sui$^-$ phenotypes were recognized by the ability to grow on medium lacking histidine (−His), whereas Ssu$^-$ phenotypes were identified by the ability to suppress the dominant His$^+$/Sui$^-$ phenotype conferred by the *SUI5* allele of eIF5 introduced on a plasmid. Adverse effects of the *IMT2* mutations on cell viability were quantified by measuring the efficiency of plating (EOP) on 5-FOA medium (Table 1; von Pawel-Rammingen et al. 1992). Viable mutants displaying significant reductions in EOP were characterized for slow-growth phenotypes (Slg$^-$) by spotting serial dilutions on +His medium (Supplemental Fig. S3).

We began by analyzing replacements of the first and third of the three consecutive G:C pairs in the ASL, unique to tRNA$_i$, with the A:U and U:U pairs found at these positions in tRNA$_e^{Met}$, generated by site-directed mutagenesis of *IMT2* (Fig. 1A). These replacements, G29A:C41U and G31U:C39U, have little effect on the EOP (Table 1) or cell growth rate (von Pawel-Rammingen et al. 1992) and do not increase growth on −His medium in the manner expected for Sui$^-$ substitutions (data not shown). However, comparing expression of matched *HIS4-lacZ* reporters containing AUG or UUG start codons revealed ~50% reduced UUG:AUG initiation ratios for both G31U:C39U and the G29A:C41U,G31U:C39U double substitution (Fig. 1B), suggesting that G31U:C39U increases initiation accuracy. This possibility is supported by the fact that G31U:C39U and the double substitution,
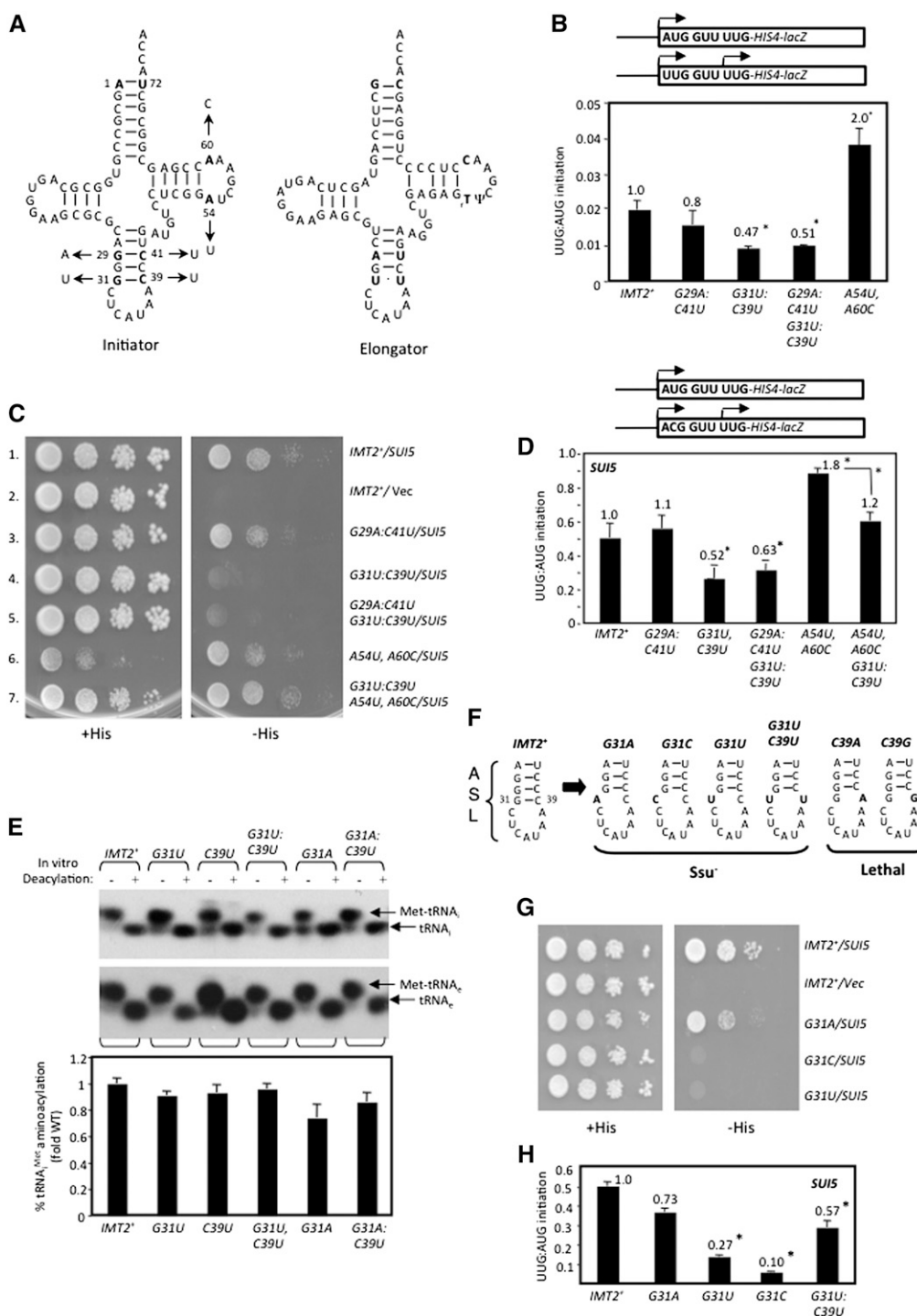
Figure 1. Loss of W:C pairing at 31:39 increases the accuracy of start codon recognition. (*A*) Secondary structures of yeast Met-tRNA$_i$ (*left*) and tRNA$_e^{Met}$ (*right*). Arrows indicate substitutions analyzed *below*. (*B*) *his4-301* strains with the indicated *IMT2* alleles and harboring *HIS4-lacZ* fusions (shown schematically) with AUG or UUG start codons (on plasmids p367 and p391, respectively) were cultured in SD+His medium, and β-galactosidase activities were measured in whole-cell extracts. Ratios of mean activities from three transformants are plotted with error bars indicating SEMs. Asterisks indicate significant differences between mutant and wild type (WT) as judged by a Student's *t*-test ($P < 0.005$). (*C*) *his4-301* strains with the indicated *IMT2* alleles and harboring a single-copy (sc) *SUI5* plasmid or empty vector (Vec) were spotted on SD+His and incubated for 3 d (+His) or 6 d (−His) at 30°C. (*D*) UUG:AUG initiation ratios were determined as in *B* for strains harboring the indicated *IMT2* alleles and sc *SUI5*, except using *HIS4-lacZ* reporters on p367 (AUG) and p4957 (UUG). Asterisks indicate significant differences between mutant and wild type or between two mutants (connected by a bracket) ($P < 0.005$). (*E*) In vivo analysis of aminoacylation. Total RNA was extracted and resolved by electrophoresis under acidic conditions and subjected to Northern analysis using [^{32}P]-labeled oligonucleotides complementary to tRNA$_i$ (*top*) or tRNA$_e^{Met}$ (*bottom*), and signal intensities were quantified by PhosphorImaging. For in vitro deacylation, an aliquot of each RNA was deacylated at pH 9.0. Normalized percentages of tRNA$_i$ aminoacylation were determined by calculating the ratio of signals Met-tRNA$_i$/(Met-tRNA$_i$ + tRNA$_i$) for each nondeacylated sample, normalizing to the same ratio determined for tRNA$_e^{Met}$, and expressing the results as a fraction of the value determined for wild type. (*F*) ASL structures and phenotypes for substitutions (in bold) at the 31:39 base pair. (*G*) Phenotypic analysis of strains with the indicated *IMT2* alleles and sc *SUI5* or empty vector conducted as in *C*. (*H*) UUG:AUG initiation ratios determined as in *D* for strains harboring the indicated *IMT2* alleles and sc *SUI5*.

Table 1. *EOP measurements of IMT2 alleles*

tRNA$_i$ substitution	Normalized EOP[a]	Growth on +His[b]	Structural element
None (wild type)	1.0	4.0+	
A1G:U72C	0.15	3.5+	Acceptor stem
G70A	0.17	1.5+	Acceptor stem
C3U:G70A	0.72	nd	Acceptor stem
G70C	0.19	1.0+	Acceptor stem
C3G:G70C	0.49	nd	Acceptor stem
G70U	1.15	nd	Acceptor stem
C3A:G70U	0.99	nd	Acceptor stem
C3A	0.36	3.0+	Acceptor stem
C3G	0.22	3.0+	Acceptor stem
C3U	0.37	3.0+	Acceptor stem
G31A:C39U	0.96	nd	ASL
G31C:C39G	0.85	nd	ASL
G31U:C39A	1.15	nd	ASL
C39U	0.33	3.5+	ASL
C39A	$<3 \times 10^{-5}$	Lethal	ASL
C39G	$<3 \times 10^{-5}$	Lethal	ASL
G31A	0.23	1.2+	ASL
G31U	0.87	nd	ASL
G31C	0.63	nd	ASL
G31U:C39U	0.89	nd	ASL
G29A:C41U G31U:C39U	0.70	nd	ASL
G29A:C41U	0.68	nd	ASL
G29U:C41A	0.80	nd	ASL
G29C:C41G	0.85	nd	ASL
G30A:C40U	0.37	4.0+	ASL
G30U:C40A	0.33	3.0+	ASL
G30C:C40G	0.70	nd	ASL
G31U:C39U A54U, A60C	0.06	1.0+	ASL, T-loop
G29A	0.85	nd	ASL
G29C	$<10^{-6}$	Lethal	ASL
G29U	0.87	nd	ASL
G30A	0.49	4.0+	ASL
G30C	$<10^{-6}$	Lethal	ASL
G30U	$<10^{-6}$	Lethal	ASL
C40A	$<10^{-6}$	Lethal	ASL
C40G	$<10^{-6}$	Lethal	ASL
C40U	1.43	nd	ASL
C41A	$<10^{-6}$	Lethal	ASL
C41G	$<10^{-6}$	Lethal	ASL
C41U	0.95	nd	ASL
A54U	$<8 \times 10^{-3c}$	Lethal	T-loop
A54C	0.56	nd	T-loop
A54G	0.49	nd	T-loop
A60U	$<1.2 \times 10^{-3c}$	Lethal	T-loop
A60C	0.77	nd	T-loop
A60G	0.56	nd	T-loop
A54U, A60C	0.17	2.5+	T-loop
A54C, A60U	0.23	4.0+	T-loop
G70U, A54U, A60C	$<2.5 \times 10^{-3}$	Lethal	Acceptor stem, T-loop
G70U, A54C, A60U	$<3.8 \times 10^{-5}$	Lethal	Acceptor stem, T-loop
G70U, A54C	$<1.2 \times 10^{-5}$	Lethal	Acceptor stem, T-loop

(nd) Not determined.

[a]Transformants of strain HD666 (harboring *IMT4*^{+}on hc *URA3* plasmid p2996) containing the indicated *IMT2* alleles on hc *LEU2* vector YEp351 were cultured to saturation in SC−Leu,−Ura, and serial dilutions were plated on YEPD medium and SC−Leu containing 1 mg/mL 5-FOA. The EOP was calculated as the ratio of colonies formed on 5-FOA medium to those formed on YEPD medium. The absolute EOP value for transformants containing wild-type *IMT2*^{+} on YEp351 (p1777) ranged from 1.1×10^{-2} to 1.6×10^{-2}, and the EOP value for each mutant was normalized to that observed for p1777.

[b]Qualitative assessment of the rate of colony formation by transformants harboring the indicated *IMT2* alleles on hc *LEU2* vector YEp351 (derived by plasmid shuffling from HD666) relative to strain HD1726 (containing wild-type *IMT2*^{+} on YEp351). Mutants harboring *IMT2* alleles that conferred an EOP of <0.4 were spotted on SD+His+Ura medium and incubated for 3 d at 30°C, and relative growth was scored qualitatively as shown in Supplemental Figure S3.

[c]EOP with *IMT2* allele on lc *LEU2* plasmid pSA03 (von Pawel-Rammingen et al. 1992).

but not G29A:C41U alone, are Ssu⁻, suppressing the His⁺ phenotype of *SUI5* (Fig. 1C, rows 1,4,5) and reducing by ~50% the elevated UUG:AUG ratio conferred by *SUI5* (Fig. 1D). (These last measurements involved a *HIS4-lacZ* UUG reporter that mimics *his4-301* in containing an ACG at codon-1 and UUG at codon-3.) Thus, converting G31:C39 to U31:U39 increases the requirement for an AUG start codon. Consistent with previous findings (von Pawel-Rammingen et al. 1992), Northern analysis of total RNA under acidic conditions shows that G31U:C39U does not diminish tRNA_i abundance or the proportion amino-acylated in vivo (Fig. 1E, seventh and eight lanes vs. first and second lanes). (Unless otherwise stated, none of the tRNA_i variants that we analyzed significantly reduce tRNA_i abundance or aminoacylation [Fig. 5A {below}; Supplemental Fig. S4A–G]).

Interestingly, any of the three possible substitutions of G31, which disrupt Watson-Crick pairing (W:C) at 31:39 (Fig. 1F), resembled G31U:C39U in conferring Ssu⁻ phenotypes, diminishing the His⁺ phenotype (Fig. 1G), and, at least for G31U and G31C, substantially lowering the elevated UUG:AUG ratio (Fig. 1H) in *SUI5* cells. The weaker Ssu⁻ phenotype of G31A might be attributable to the fact that it introduces an A:C wobble pair at 31:39. Although G31A evokes a 20%–30% reduction in the proportion of tRNA_i aminoacylated in vivo (Fig. 1E), this is unlikely to contribute to its Ssu⁻ phenotype because a strain lacking two of four *IMT* genes (*IMT3* and *IMT4*), with substantially reduced levels of tRNA_i and TC (Dever et al. 1995), displays essentially wild-type UUG:AUG initiation (Supplemental Fig. S5). C39A and C39G, which also disrupt W:C pairing at 31:39, are lethal (Table 1; Fig. 1F). These findings are consistent with the possibility that W:C pairing at 31:39 is important for efficient start codon recognition such that viable Ssu⁻ substitutions disrupting 31:39 increase the requirement for AUG and thereby diminish UUG initiation. In this view, the lethal substitutions would substantially reduce recognition of AUG as well as near-cognates.

We also examined the effects of disrupting W:C pairing at G29:C41 and G30:C40. As summarized in Figure 2F, seven of eight single-base substitutions that introduce purine: purine or pyrimidine:pyrimidine pairs at positions 29:41 or 30:40 are lethal. In contrast, substitutions that generate A:C or G:U wobble replacements are viable and either have no effect on initiation accuracy (G29A, G30A, and C40U) or moderately increase accuracy and confer a weak Ssu⁻ phenotype (C41U) (Table 1; Supplemental Fig. S6A–E).

Thus, the integrity of all three G:C base pairs in the ASL stem is critical in vivo, as substitutions that generate purine:purine pairs at any of these positions are lethal, and pyrimidine:pyrimidine pairs are either lethal (first and second base pairs) or confer marked hyperaccuracy (Ssu⁻) phenotypes (third base pair). In contrast, most wobble replacements appear to have little or no effect on initiation accuracy.

## W:C substitutions of 31:39 in the ASL strongly decrease initiation accuracy

We next analyzed the effects of double substitutions that replace the conserved G:C base pairs with other W:C pairs (Fig. 2A). Remarkably, all three W:C replacements of G31:C39 as well as C39U, which produces a wobble G:U at this position, substantially reduce initiation accuracy, conferring His⁺/Sui⁻ phenotypes (Fig. 2B) and increasing the UUG:AUG ratio sixfold to sevenfold for the W:C substitutions and ~2.5-fold for the G:U replacement (Fig. 2C). In contrast, W:C substitutions of the first G:C pair did not produce His⁺ phenotypes (Fig. 2D; data not shown) and evoked <30% increases in the UUG:AUG ratio (Fig. 2E). W:C replacements of the second G:C pair conferred somewhat greater increases in the UUG:AUG ratio (Fig. 2E) and a His⁺ phenotype only for G30C:C40G (Fig. 2D). As noted above, C40U and C41U substitutions that introduce G:U wobble pairs at 29:41 and 30:40 do not confer Sui⁻ phenotypes (Fig. 2F). Thus, W:C substitutions at each of the ASL G:C pairs reduce initiation accuracy, with the strongest defects for the 31:39 substitutions adjacent to the anticodon loop and the weakest defects for the 29:41 substitutions furthest from the anticodon loop (Fig. 2A). One way to explain these findings is to propose that the ASL G:C pairs promote initiation accuracy by affecting the conformation of the anticodon loop, with the 31:39 pair closest to the loop having the greatest effect on accuracy.

Ssu⁻ disruptions of 31:39 destabilize the closed/P_IN conformation of the PIC

The fact that G31C and G31U evoke Ssu⁻ phenotypes suggests that these mutations destabilize the closed/P_IN state of the PIC normally triggered by start codon recognition (Supplemental Fig. S2C). To test this interpretation, we examined the effects of these substitutions on the equilibrium and rate constants governing TC binding to the 40S subunit. We first determined that [³⁵S]-Met-tRNA_i variants harboring these substitutions all efficiently form TC with eIF2 and GDPNP (Supplemental Table S1). Subsequently, we measured the affinities of the TCs for the 40S subunit in the presence of saturating eIF1, eIF1A, and a model mRNA containing an AUG or UUG start codon using native gel electrophoresis to separate bound and unbound fractions of TC. Interestingly, G31C and G31U increased the affinity of TCs for 40S complexes lacking mRNA while greatly reducing affinity in the presence of mRNA(AUG) (Fig. 3A; Table 2). Strikingly, the affinity of these mutant TCs for the 43S·mRNA(UUG) complex is so low that no complex formation could be detected at the highest concentrations of 40S subunits employed (≥250 nM) (Table 2; data not shown). These findings support the prediction that G31C and G31U destabilize the closed/P_IN state, and the fact that TC affinity is much lower for the UUG versus AUG complex is consistent with the Ssu⁻ phenotype of these mutations (Fig. 1H). Moreover, considering that the wild-type TC has a much lower affinity for 43S versus 43S·mRNA(AUG) complexes (Table 2; Kapp et al. 2006), the fact that G31C/G31U essentially eliminate this differential in stability indicates that they abolish thermodynamic coupling between Met-tRNA_i and the start codon.

We previously proposed that the endpoints of curves for TC binding at high concentrations of 40S subunits reflect
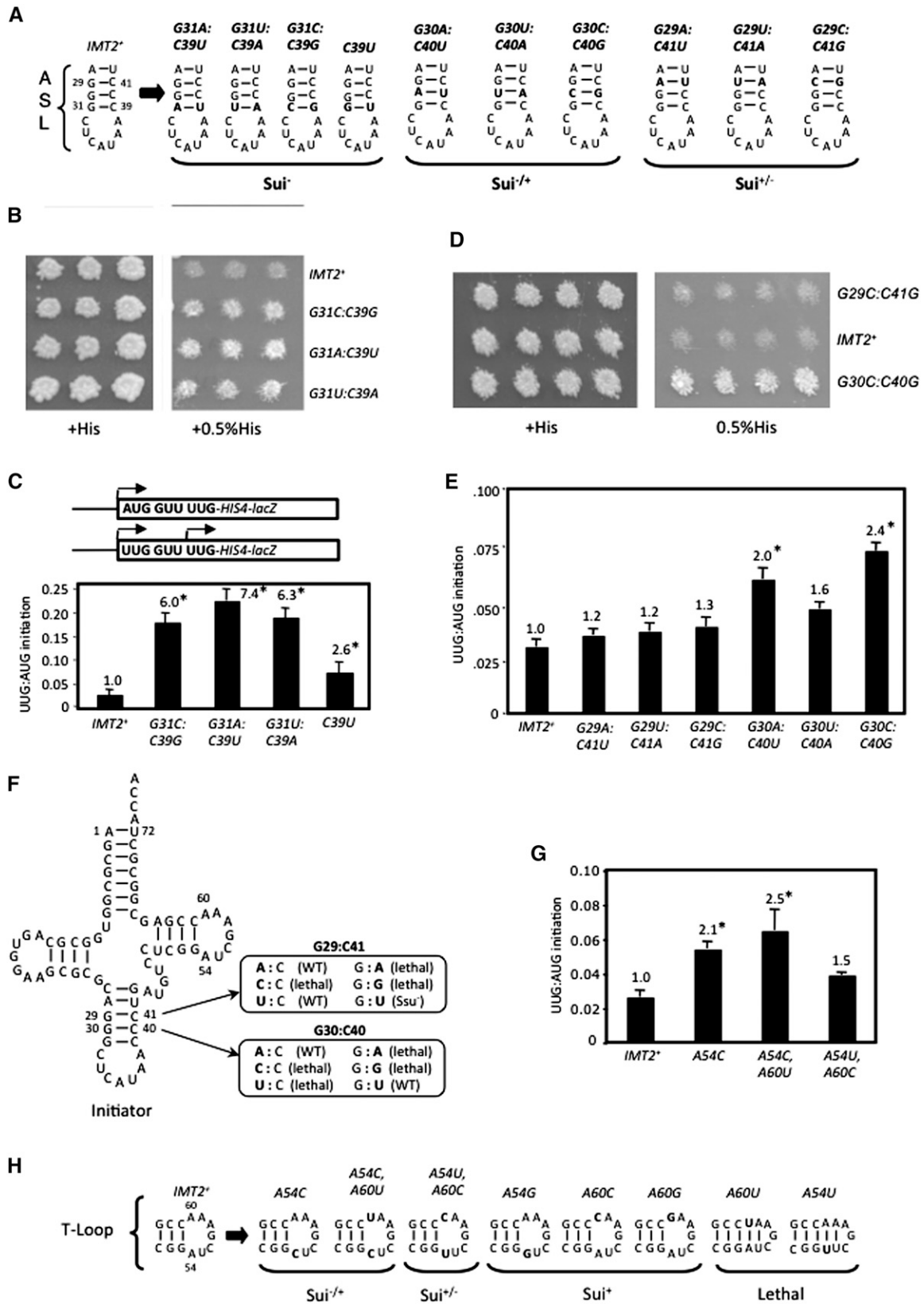
Figure 2. W:C replacements at 31:39 and A54 substitutions in the T-loop reduce the accuracy of start codon recognition. (*A*) ASL structures and phenotypes (in order of severity: Sui⁻ > Sui⁻/⁺ > Sui⁺/⁻) for W:C substitutions of G:C pairs. (*B,D*) *his4-301* strains with the indicated *IMT2* alleles were replica-plated to +His medium (0.3 mM His) or 0.5% His (1.5 μM His) and incubated for 3 d (+His) or 7–10 d (0.5% His). (*C,E,G*) UUG:AUG initiation ratios were determined as in Figure 1B for strains with the indicated *IMT2* alleles. (*F*) Phenotypes of substitutions that disrupt W:C pairing at positions 29:41 and 30:40. (*H*) Structures of the T-loop with substitutions at A54 or A60 and the associated phenotypes.
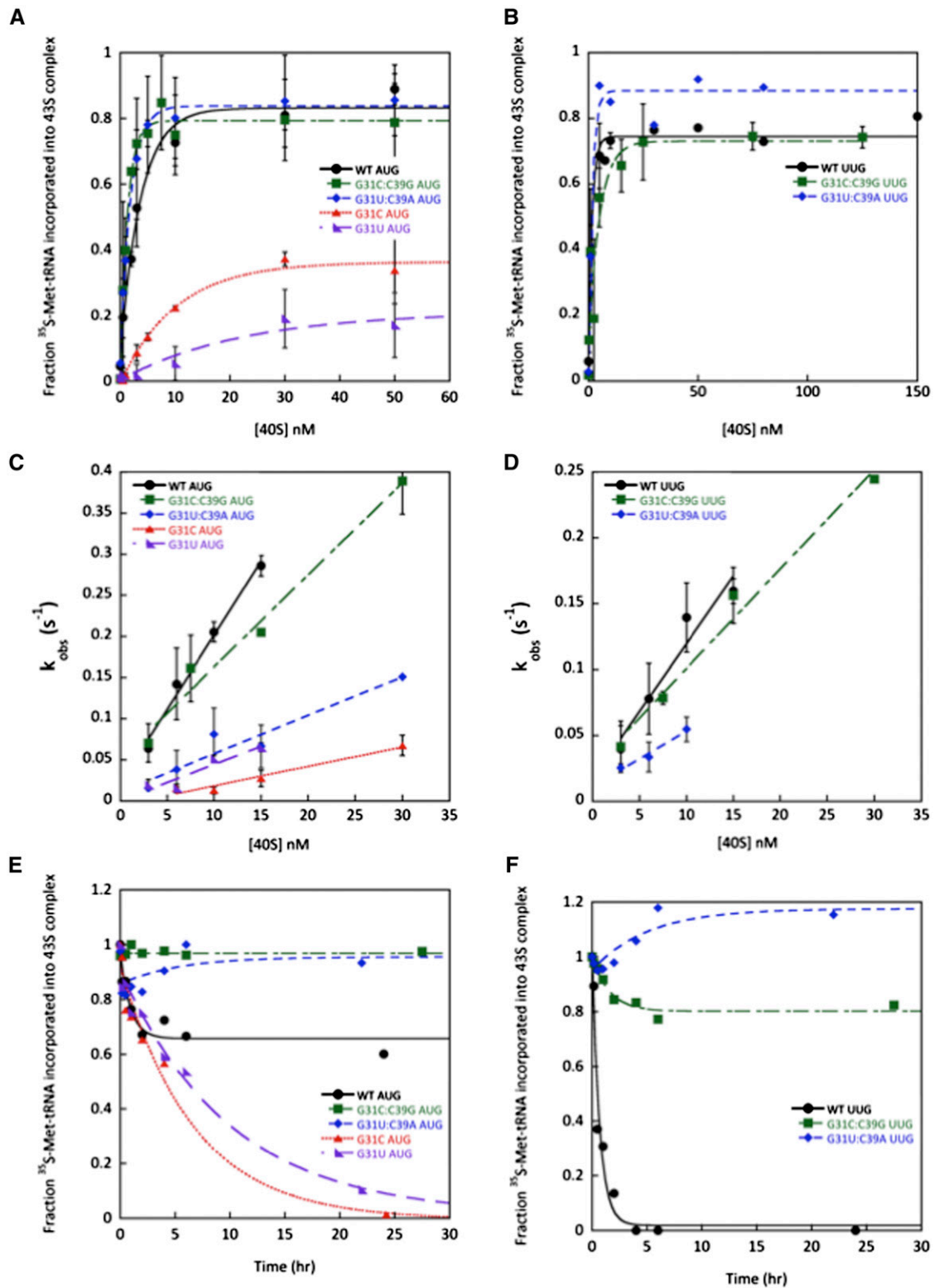
Figure 3. Disrupting ASL base pair G31:C39 and replacing it with other W:C base pairs have opposite effects on the stability of 43S·mRNA complexes. (A,B) Determination of K_d values for TC (with wild-type [WT] or the indicated variant of [^{35}S]-Met-tRNA$_i$) binding to 40S•eIF1•eIF1A complexes assembled with mRNA(AUG) (A) or mRNA(UUG) (B). (C,D) Determination of k_{on} values for TC binding to 40S•eIF1•eIF1A complexes from plots of observed rate constants (k_{obs}) versus 40S concentration with mRNA(AUG) (C) or mRNA(UUG) (D). (E,F) Analysis of TC dissociation from 43S•mRNA complexes for mRNA(AUG) (E) or mRNA(UUG) complexes (F). Representative curves from at least two independent experiments are shown. k_{off} values and end-points for dissociable complexes are given in Supplemental Table S2.

Table 2. *Affinity of TC for 40S·eIF1·eIF1A·mRNA complexes*

| Phenotype | tRNA$_i$ | K_d | | | Endpoint (fraction bound) | | |
		(A) No mRNA	(B) +mRNA (AUG)	(C) +mRNA (UUG)	(D) No mRNA	(E) +mRNA (AUG)	(F) +mRNA (UUG)
	Wild type	60 mM ± 5 mM	≤1 nM	≤1 nM	0.47 ± 0.14	0.85 ± 0.09	0.80 ± 0.10
Ssu⁻	G31C	29 mM ± 15 mM	11 nM ± 2 nM	>250 nM	0.28 ± 0.10	0.29 ± 0.16	n/a
Ssu⁻	G31U	18 mM ± 10 mM	34 nM ± 4 nM	>250 nM	0.25 ± 0.06	0.23 ± 0.06	n/a
Sui⁻ Gcd⁺	G31C:C39G	38 mM ± 23 mM	≤1 nM	≤1 nM	0.35 ± 0.19	0.81 ± 0.14	0.77 ± 0.05
Sui⁻ Gcd⁺	G31U:C39A	41 mM	≤1 nM	≤1 nM	0.44	0.86 ± 0.07	0.93 ± 0.05
Sui⁻ Gcd⁻	G70A	33 mM ± 7 mM	≤1 nM	≤1 nM	0.58 ± 0.01	0.76 ± 0.06	0.68 ± 0.18
Sui⁻/⁺	C3U:G70A	25 mM ± 11 mM	≤1 nM	≤1 nM	0.74 ± 0.20	0.91 ± 0.06	0.80 ± 0.05

Values are the averages of at least two independent experiments with the exception of G31U:C39A in the absence of mRNA. Errors are average deviations.

the distribution of PICs in the open versus closed states; the open state was proposed to be unstable during electrophoresis and therefore could not be visualized, leading to endpoints of less than one (measured as fractions of TC bound to 40S complexes) in cases where open complex persists (Kapp et al. 2006; Kolitz et al. 2009). Consistent with this idea, G31C and G31U, which we propose bias the system toward the open/P$_{OUT}$ state, decrease the endpoints of TC binding in both the absence and presence of mRNA(AUG) (Fig. 3A; Table 2).

To gain more insight into the effect of these mutations on formation and stability of the PIC, we measured the rate constants for TC forming and dissociating from PICs. The kinetics of TC binding was measured by mixing TC containing [³⁵S]-Met-tRNA$_i$ with varying concentrations of 40S subunits and saturating eIF1, eIF1A, and mRNA(AUG) or mRNA(UUG). Time points were removed, reactions were terminated with excess unlabeled TC, and the amount of labeled TC in PICs was measured by native gel electrophoresis. The slope of the plot of the pseudo-first-order rate constants (k_{obs}) for PIC formation versus 40S concentration yields the second-order rate constant (k_{on}) (Kolitz et al. 2009).

The G31C and G31U mutations decrease k_{on} for TC in the presence of mRNA(AUG) by eightfold and fourfold, respectively (Fig. 3C; Table 3). The corresponding values with mRNA(UUG) could not be determined because TC binding with these mutants is too weak to measure. One possible interpretation of these data is that the mutations

slow conversion of the open/P$_{OUT}$ state of the PIC to the closed/P$_{IN}$ state, which is dramatically accelerated by start codon recognition in wild-type PICs and has a strong influence on the observed rate of PIC formation (Kolitz et al. 2009). Slowing of this step would be consistent with the mutants' Ssu⁻ phenotypes.

Next, we measured the rate at which TC made with the mutant tRNAs dissociates from PICs. After assembling 43S·mRNA complexes as above, we quantified the amount of [³⁵S]-Met-tRNA$_i$ remaining in the slowly migrating PIC band as a function of time after adding a chase of excess unlabeled TC made with wild-type Met-tRNA$_i$. With wild-type PICs formed with mRNA(AUG), TC dissociates from ~40% of the PICs with a rate constant of 0.4 h^{-1}, whereas the remaining ~60% of the complexes are completely stable over this time period (Fig. 3E). We presume that the former fraction of PICs contain Met-tRNA$_i$ bound in the P$_{IN}$ state, whereas the latter arise by isomerization of Met-tRNA$_i$ from P$_{IN}$ to a new state where it is fully locked in to the P site. This putative highly stable state might be closer to the classical P/P state than the P/I state observed recently in reconstituted mammalian PICs (Hashem et al. 2013; Lomakin and Steitz 2013), which can be regarded as the P$_{IN}$ conformation. (As the AUG codon-dependent conversion to the initial closed/P$_{IN}$ state is rapid [Kolitz et al. 2009], it is unlikely that the two states represent open/P$_{OUT}$ and closed/P$_{IN}$ because if the rate of reversion of the closed/P$_{IN}$ state back to the open/P$_{OUT}$ state was slow, all of the complexes should be in the

Table 3. *Rate constants for TC association with 40S·eIF1·eIF1A·mRNA complexes*

| tRNA$_i$ | eIF1A | k_{on} | |
		(A) +mRNA(AUG)	(B) +mRNA(UUG)
Wild type	Wild type	18.0×10^6 M^{-1}s^{-1} ± 0.2×10^6 M^{-1}s^{-1}	11.6×10^6 M^{-1}s^{-1} ± 0.1×10^6 M^{-1}s^{-1}
G31C	Wild type	2.3×10^6 M^{-1}s^{-1} ± 0.2×10^6 M^{-1}s^{-1}	n/a
G31U	Wild type	4.4×10^6 M^{-1}s^{-1} ± 0.2×10^6 M^{-1}s^{-1}	n/a
G31C:C39G	Wild type	9.1×10^6 M^{-1}s^{-1} ± 2.9×10^6 M^{-1}s^{-1}	5.1×10^6 M^{-1}s^{-1} ± 1.8×10^6 M^{-1}s^{-1}
G31U:C39A	Wild type	5.6×10^6 M^{-1}s^{-1} ± 0.4×10^6 M^{-1}s^{-1}	3.7×10^6 M^{-1}s^{-1} ± 1.3×10^6 M^{-1}s^{-1}
G70A	Wild type	0.7×10^6 M^{-1}s^{-1} ± 0.4×10^6 M^{-1}s^{-1}	7.5×10^6 M^{-1}s^{-1} ± 0.9×10^6 M^{-1}s^{-1}
C3U:G70A	Wild type	7.1×10^6 M^{-1}s^{-1} ± 2.6×10^6 M^{-1}s^{-1}	11.6×10^6 M^{-1}s^{-1} ± 0.5×10^6 M^{-1}s^{-1}
G70A	17-21	43.0×10^6 M^{-1}s^{-1} ± 1.2×10^6 M^{-1}s^{-1}	3.3×10^6 M^{-1}s^{-1} ± 1.3×10^6 M^{-1}s^{-1}
Wild type	17-21	4.7×10^6 M^{-1}s^{-1} ± 0.3×10^6 M^{-1}s^{-1}	10.1×10^6 M^{-1}s^{-1} ± 0.7×10^6 M^{-1}s^{-1}

Values are the averages of at least two independent experiments. Errors are average deviations. (n/a) Not applicable.

closed/P_{IN} state, whereas if the rate of reversion was fast, all of the complexes should dissociate on chasing with unlabeled TC.) Importantly, dissociation of wild-type TC from PICs assembled on mRNA(UUG) goes to completion and occurs with a rate constant of 1.2 h^{-1} (Fig. 3F), suggesting that PICs do not achieve the highly stable state with a UUG codon in the P site.

Interestingly, both G31C and G31U increase the fraction of AUG complexes from which TC can dissociate, from ~40% with wild type to 100% with the mutants (Fig. 3E), resembling the behavior of wild-type complexes at UUG (Fig. 3F). Thus, the Ssu$^-$ mutations decrease the ability of the PIC to enter the highly stable state accessible to the wild-type complex.

Sui$^-$ W:C substitutions of 31:39 stabilize the closed/P_{IN} state

As described above, the Ssu$^-$ phenotypes of the G31C and G31U mutations in the ASL are suppressed by the compensatory C39G and C39A mutations that restore W:C pairing at this position; and these double mutants produce Sui$^-$ phenotypes instead, suggesting that they shift the balance in favor of the closed/P_{IN} state. Consistent with this proposal, G31C:C39G and G31U:C39A dramatically reduce the K_ds for TC binding to the 40S complex with both mRNA(AUG) and mRNA(UUG) relative to the K_ds with the G31C and G31U single substitutions and also restore the endpoints of TC binding (Fig. 3A,B; Table 2). These data suggest that the double mutations stabilize the closed/P_{IN} state.

Analysis of dissociation kinetics revealed that G31C:C39G and G31U:C39A produce complexes from which >80% of the TC does not dissociate with mRNA(AUG) or mRNA(UUG) (Fig. 3E,F), indicating that they not only favor the closed/P_{IN} state but lead to more complexes entering the highly stable state. The magnitude of these changes appear to be bigger with mRNA(UUG) (Fig. 3E,F, cf. curves for wild type vs. G31C:C39G and G31U:C39A), consistent with the elevated UUG:AUG initiation ratios observed in vivo for these variants.

Analysis of association kinetics showed that the k_{on} value in the presence of mRNA(AUG) with the G31C:C39G mutant was increased fourfold relative to that with G31C (Fig. 3C; Table 3), suggesting that restoring this base pair speeds up conversion of the open/P_{OUT} state to the closed/P_{IN} state on start codon recognition. The G31U:C39A mutation does not enhance the rate of TC loading relative to that seen with the Ssu$^-$ G31U mutant, however (Fig. 3C; Table 3), suggesting that the key effect of the Sui$^-$ mutations is on stability of the closed/P_{IN} state, which is reflected in the dissociation rates. Stable complexes could not be formed on mRNA(UUG) with the G31C and G31U mutants, but restoring base-pairing at position 31:39 restores stable complex formation, as noted above. The k_{on} values for mRNA(UUG) complexes with the G31C:C39G and G31U:C39A mutants were twofold to threefold lower than with wild type (Fig. 3D; Table 3), but because k_{on} values could not be measured with the single

mutants, we cannot determine the extent to which restoring the base pair increases k_{on}.

T-loop residue A54 contributes to stringent AUG selection

The results described above indicate that Ssu$^-$ substitutions G31C and G31U destabilize TC binding to 43S·mRNA complexes in vitro (Table 2). We observed the same outcome previously on replacing G31:C39 with the U:U pair found in tRNA$_e$^{Met} (Kapp et al. 2006), and, importantly, we concluded above that G31U:C39U likewise confers an Ssu$^-$ phenotype in vivo (Fig. 1B–D). We also reported that substitutions A54U and A60C of the two signature T-loop residues of tRNA$_i$ reduced the deleterious effect of G31U:C39U on the affinity of TC for 43S·mRNA(AUG) complexes (Kapp et al. 2006). We reasoned that if the Ssu$^-$ phenotype of G31U:C39U results from less stable binding of Met-tRNA$_i$ to the closed/P_{IN} state of the PIC, as proposed above for G31C and G31U, then the A54U,A60C substitutions should suppress the Ssu$^-$ phenotype of G31U:C39U.

Remarkably, combining A54U,A60C with G31U:C39U restores the His$^+$ phenotype (Fig. 1C, cf. rows 4,7 vs. row 1) and reinstates the elevated UUG:AUG ratio conferred by *SUI5* in *IMT2*$^+$ cells (Fig. 1D, cf. columns 3,6 vs. column 1). A54U,A60C also produces a modest Sui$^-$ phenotype in otherwise wild-type cells, increasing the UUG:AUG ratio (Fig. 1B). Consistent with this, A54U,A60C exacerbates the Sui$^-$ phenotype of *SUI5*, decreasing growth on +His but not −His medium (Fig. 1C, rows 1,6) and elevating the UUG:AUG ratio above that seen in *SUI5 IMT2*$^+$cells (Fig. 1D, columns 1,5). Note also that G31U:C39U reverses the Slg$^-$ phenotype of the A54U,A60C substitution in *SUI5* cells on +His medium (Fig. 1C, +His, rows 1,6,7), which likely reflects the ability of G31U:C39U to mitigate the elevated UUG initiation conferred by A54U,A60C in *SUI5* cells (Fig. 1D, columns 5,6). Thus, replacing both highly conserved T-loop residues with the corresponding bases in tRNA$_e$^{Met} decreases the accuracy of AUG selection (Sui$^-$) and suppresses the hyperaccurate (Ssu$^-$) phenotype of the ASL substitution G31U:C39U, and these substitutions mutually suppress their opposing effects on initiation accuracy. The fact that A54U,A60C suppresses the destabilizing effect on TC binding to 43S·mRNA PICs in vitro (Kapp et al. 2006) as well as the Ssu$^-$ phenotype of G31U:C39U in cells (Fig. 1C,D) provides strong evidence that the stability of the closed/P_{IN} state of the PIC is a critical determinant of initiation accuracy in vivo.

We went on to explore which T-loop substitution confers the moderate Sui$^-$ phenotype of A54U,A60C. Neither A60C nor A60G single substitutions affected the UUG:AUG ratio (summarized in Fig. 2H; data not shown). These findings, together with the fact that A54C alone confers a Sui$^-$ phenotype (Fig. 2G), suggest that A54U is responsible for the Sui$^-$ phenotype of A54U,A60C. However, we cannot eliminate the possibility that A60C contributes to the Sui$^-$ phenotype of the A54U,A60C double mutant. Interestingly, both A54U and A60U are lethal (Table 1), which might derive from their ability to

extend the T-stem as depicted in Figure 2H. However, A54C alone or in combination with A60U increases the UUG:AUG ratio by a factor of 2.0–2.5 (Fig. 2G), whereas A54G does not significantly affect the UUG:AUG ratio (data not shown). We conclude that a purine residue is required at position 54 in the T-loop for wild-type discrimination against UUG start codons.

Acceptor stem residue G70 is crucial for stringent AUG selection

To identify additional determinants of initiation accuracy, we screened a library of mutant *IMT2* plasmids produced by random mutagenesis for a His[+] phenotype in the *his4-301* strain and identified the G70U substitution in the acceptor stem as a novel Sui[−] mutation (Fig. 4C [−His, rows 1,2], D [columns 1,6]). C3:G70 is a highly conserved feature of tRNA$_i$ in all kingdoms of life (Marck and Grosjean 2002), but its possible function in initiation was unknown. Interestingly, site-directed mutagenesis showed that G70A, G70C, and C3G confer even stronger His[+]/Sui[−] phenotypes (Fig. 4C) and larger (ninefold or greater) increases in UUG:AUG initiation compared with G70U (Fig. 4D). However, C3A and C3U confer smaller increases in the UUG:AUG ratio (~2.5-fold) (Fig. 4D) and little growth on −His medium (Fig. 4C). The strength of the His[+]/Sui[−] and elevated UUG:AUG initiation phenotypes of these substitutions (Fig. 4C [−His], D) correlate well with their effects on cell growth (Fig. 4C, +His). Thus, disrupting W:C pairing at 3:70 confers a Sui[−] phenotype whose severity varies with the substitution (summarized in Fig. 4A).

C3U, which introduces a U:G wobble pair (Fig. 4A), produces one of the weakest Sui[−] phenotypes among the single-base changes in the 3:70 base pair (Fig. 4C,D). Consistent with this, combining C3U with G70A to introduce a W:C replacement at the 3:70 base pair (Fig. 4A) effectively diminishes the Slg[−], His[+], and elevated UUG:AUG initiation phenotypes conferred by G70A (Fig. 4B–D). Similar findings were obtained when G70C and G70U were combined with the appropriate C3 substitutions to reinstate W:C pairing, although suppression of the strong Sui[−] phenotypes of G70C and G70U was less pronounced, as the double substitutions retained weak His[+] phenotypes and significantly elevated UUG:AUG ratios (Fig. 4A–D). Nevertheless, it is noteworthy that combining these mutations mitigated rather than exacerbated their respective Sui[−]/Slg[−] phenotypes. We conclude that base-pairing per se and the identity of the W:C pair at position 3:70 both contribute to discrimination against UUG start codons.

*C3:G70 substitutions confer Gcd[−] phenotypes without decreasing TC abundance in vivo*

Interestingly, we found that the Sui[−] substitutions at C3:G70 confer constitutive derepression of a *GCN4-lacZ* reporter, the Gcd[−] phenotype, indicating a reduced rate of TC binding to 40S subunits in vivo. A decrease in the rate of TC binding to 40S subunits derepresses *GCN4-lacZ* expression because scanning 40S subunits that have

already translated uORF1 can bypass the start codons of the inhibitory uORF2–4 before rebinding TC and then reinitiate further downstream at the *GCN4* AUG codon instead (Hinnebusch 2005). Whereas G70A, G70C, G70U, C3A, and C3G, all disrupting C3:G70, confer twofold to threefold increases in *GCN4-lacZ* reporter expression in nonstarvation conditions, the C3U:G70 wobble substitution and C3U:G70A, C3G:G70C, and C3A:G70U double substitutions (producing W:C replacements) have smaller (<1.7-fold) effects on *GCN4-lacZ* expression (Fig. 4E). In particular, C3U:G70A suppresses the marked derepression of *GCN4-lacZ* conferred by G70A (Fig. 4E, columns 2,3). None of the G70 or C3 single substitutions significantly affected expression of a *GCN4-lacZ* reporter lacking all four uORFs (Supplemental Fig. S7A), indicating that they alter translational control of *GCN4-lacZ* expression. The severity of the Gcd[−] phenotypes provoked by disrupting or altering C3:G70 is generally correlated with that of the Sui[−] phenotypes produced by these mutations (Fig. 4, cf. D and E), suggesting that these defects are mechanistically linked. Moreover, none of the strong Sui[−] substitutions involving W:C replacements of G31:C39 confers a Gcd[−] phenotype (Supplemental Fig. S7B), suggesting distinct mechanisms underlying the Sui[−] phenotypes of 31:39 versus 3:70 substitutions.

Importantly, none of the Gcd[−] G70 substitutions (G70A, G70C, and G70U) reduces tRNA$_i$ abundance (Supplemental Fig. S4E) or tRNA$_i$ aminoacylation in vivo (Fig. 5A; data not shown). Given the location of C3:G70 in the acceptor stem, which contacts eIF2 (Shin et al. 2011), G70 substitutions might reduce TC formation as the means of derepressing *GCN4* translation. In fact, our in vitro measurements of Met-tRNA$_i$ binding to eIF2 revealed approximately fourfold increases in K_d for C3U and G70A that were mitigated in the C3U:G70A double mutant (Supplemental Table S1). Accordingly, we measured native TC levels in cell extracts by immunoprecipitating Flag-tagged eIF2β (FL-Sui3) expressed in the *IMT2* mutants of interest, probed immune complexes by Northern analysis for tRNA$_i$ levels, and normalized the tRNA$_i$ signal for amounts of immunoprecipitated FL-Sui3 (Fig. 5B–D). We verified that only a low background level of tRNA$_i$ was immunoprecipitated from the parental *IMT2*^{+} strain containing untagged eIF2β (Fig. 5C,D, [−]tag) and that the eIF2γ-N135D substitution (Alone et al. 2008) reduces the amount of tRNA$_i$ coimmunoprecipitating with eIF2β-FL (Supplemental Fig. S8A–C). Using this assay, we observed no difference between wild type and the G70U, G70A, and G70C mutants (Fig. 5B–D), suggesting that G70 substitutions do not significantly reduce TC abundance in vivo. Accordingly, their Gcd[−] phenotypes likely result instead from reducing the rate of TC binding to 40S subunits scanning downstream from uORF1, which induces reinitiation at *GCN4* (Hinnebusch 2005).

eIF1A mutation 17-21 cosuppresses Sui[−] and Gcd[−] phenotypes of C3:G70 substitutions

We showed previously that mutations in the SEs of the eIF1A CTT confer Sui[−] and Gcd[−] phenotypes that are
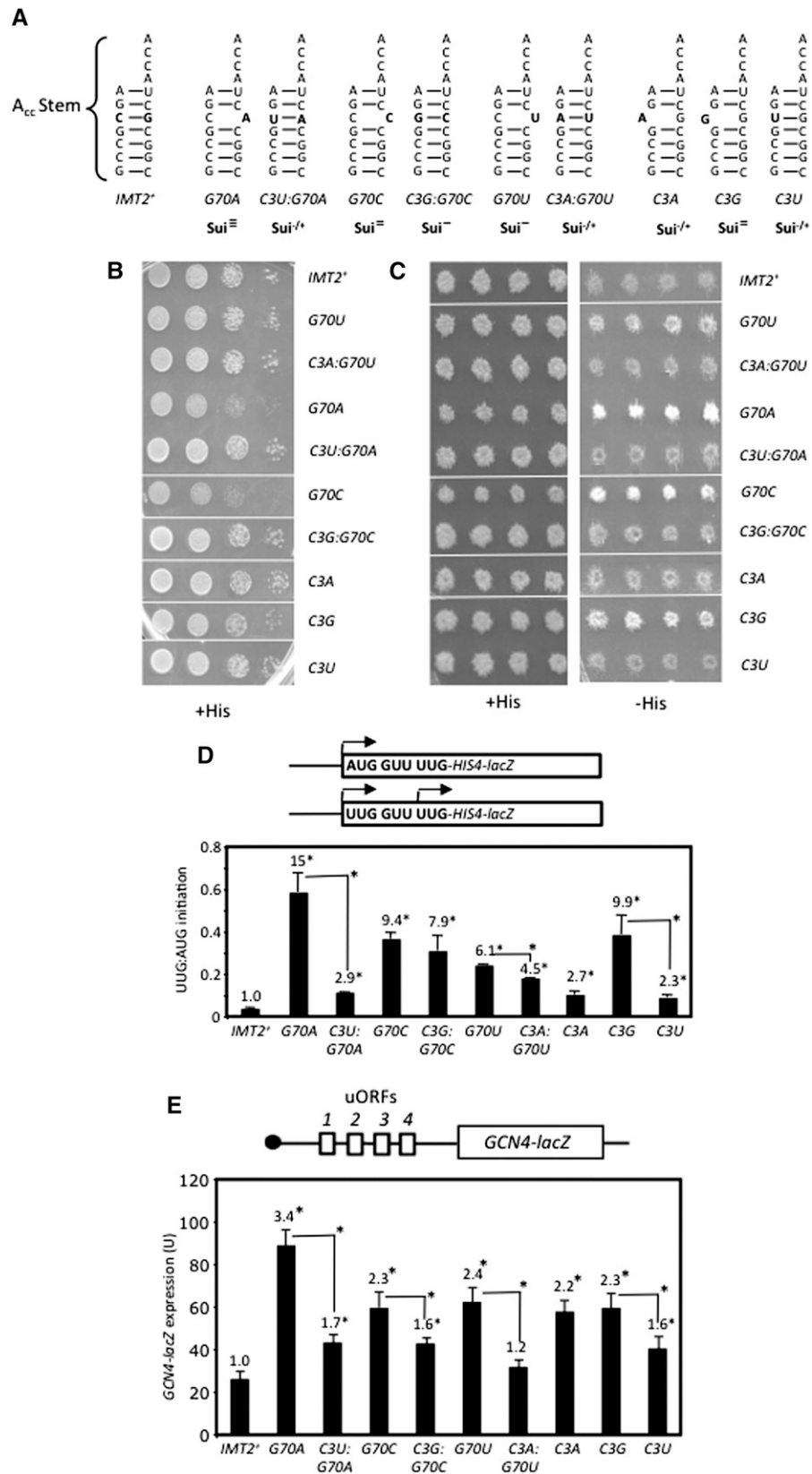
Figure 4. C3:G70 in the acceptor stem is crucial for accurate AUG selection and rapid TC binding to PICs in vivo. (*A*) Acceptor stem structures and phenotypes (in order of severity: Sui³⁻ > Sui²⁻ > Sui⁻ > Sui⁻/⁺) for 3:70 substitutions. (*B*) Slg⁻ phenotypes on +His medium analyzed as in Figure 1C. (*C*) His⁺/Sui⁻ phenotypes analyzed as in Figure 2B. (Results in *B* and *C* were obtained in parallel from the same plates and rearranged only for ease of interpretation.) (*D*) UUG:AUG initiation ratios were determined as in Figure 1B. (*E*) β-Galactosidase expressed from the *GCN4-lacZ* reporter on p180 measured as in Figure 1B.
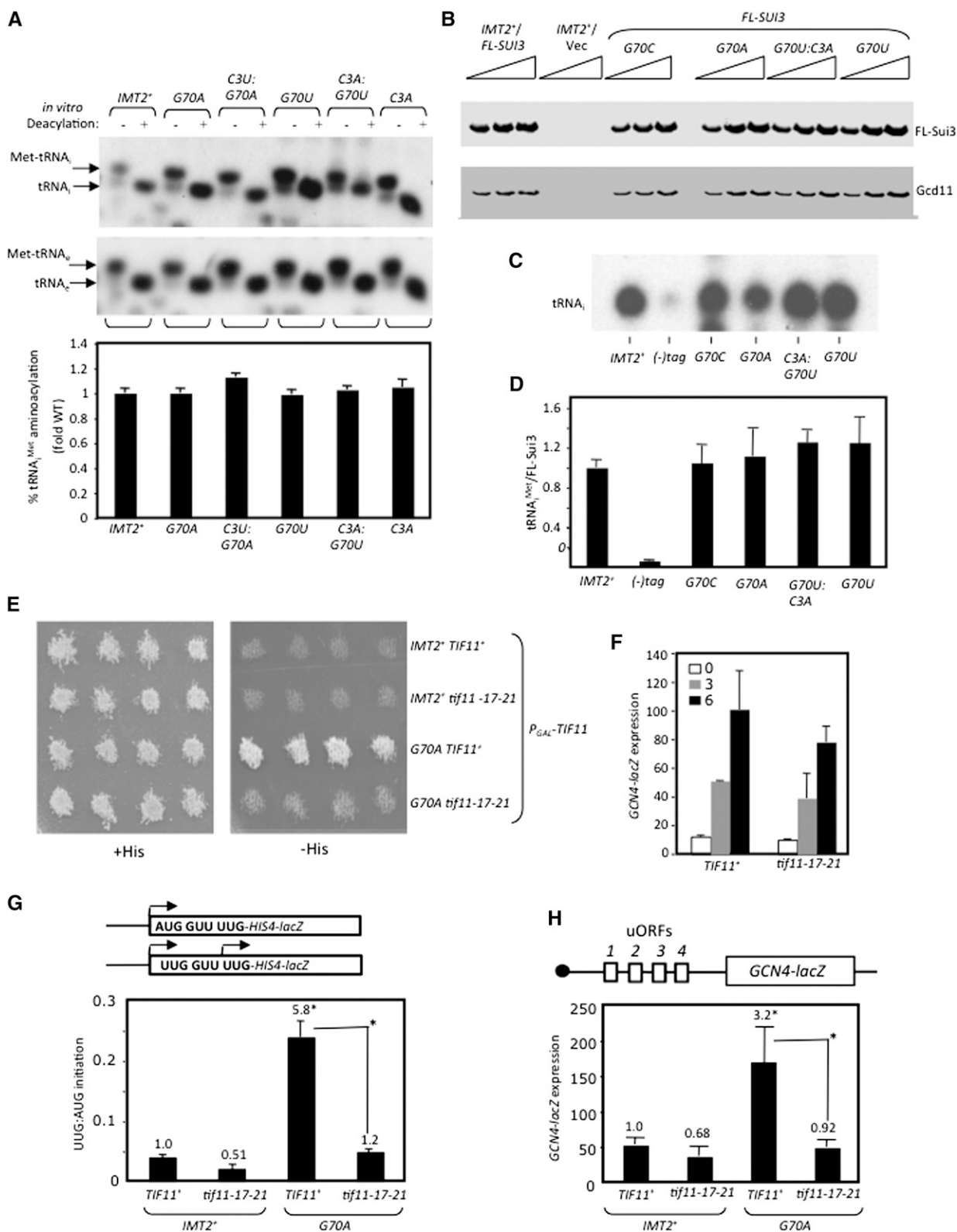
Figure 5. Evidence that the Sui⁻ and Gcd⁻ phenotypes of the G70A substitution have a common molecular basis. (*A*) Substitutions of C3:G70 do not affect aminoacylation in vivo. Analysis conducted as in Figure 1E. (*B–D*) Substitutions of C3:G70 do not impair TC assembly in vivo. (*B*) Whole-cell extracts from strains harboring a *SUI3-FL* plasmid or empty vector were immunoprecipitated with Flag antibodies, and 5% of each immune complex was subjected to Western analysis with Flag or Gcd11/eIF2β antibodies. (*C*) RNA extracted from the remainder was subjected to Northern analysis of tRNA$_i$. The second lane in *C* derives from the *IMT2⁺* strain with untagged *SUI3*; all others derive from *SUI3-FL* strains. Northern signals in *C* quantified by PhosphorImaging were normalized for FL-Sui3/ eIF2β Western signals in *B* and quantified with the Odyssey Infrared imaging system, and the resulting ratios were normalized to those determined for the *IMT2⁺SUI3-FL* strain. Mean ratios and SEMs from three independent immunoprecipitations were plotted. (*E*) *his4-301* strains harboring chromosomal P_{GAL1}-*TIF11* and plasmid-borne *TIF11⁺* or *tif11-17-21* and the indicated *IMT2* allele analyzed as in Figure 2B. (*F*) *GCN4-lacZ* expression was assayed in cells cultured in SD+His ("0") or with 1 mg/L sulfometuron methyl (SM) for 3 h or 6 h. (*G*) UUG:AUG initiation ratios were determined as in Figure 1B. (*H*) *GCN4-lacZ* expression was measured as in Figure 1B.

cosuppressed by the Ssu⁻ mutation *17-21* in the SI element of the eIF1A NTT. This and other findings led us to conclude that SE mutations destabilize the open conformation of the 40S subunit and P_{OUT} mode of TC binding. Destabilization of the open/P_{OUT} state reduces the rate of TC binding and confers the Gcd⁻ phenotype, as TC binds most rapidly to the open conformation and also shifts the balance from the open/P_{OUT} to closed/P_{IN} state to permit more frequent initiation at UUG codons for the Sui⁻ phenotype (Supplemental Fig. S2B). The *17-21* substitution suppresses both defects by stabilizing the open/P_{OUT} state, restoring rapid TC loading and maintaining the scanning-conducive conformation at UUG codons (Supplemental Fig. S2C; Saini et al. 2010).

Thus, it was of interest to determine whether the *17-21* mutation can also cosuppress the Sui⁻ and Gcd⁻ phenotypes of the G70A substitution. To this end, we constructed strains in which expression of wild-type eIF1A from a chromosomal P_{GAL1}-*TIF11* allele is repressed on glucose medium, and either the wild-type or 17-21 forms of eIF1A are expressed constitutively from plasmid-borne alleles under the native promoter. Remarkably, the His⁺/Sui⁻ phenotype (Fig. 5E) and elevated UUG:AUG initiation ratio (Fig. 5G) as well as the Gcd⁻ phenotype (Fig. 5H) conferred by *G70A* were essentially eliminated in the *tif11-17-21* strain. This cosuppression of G70A phenotypes suggests that, like eIF1A SEs, the C3:G70 base pair preferentially stabilizes the open/P_{OUT} conformation of the PIC.

We also demonstrated that *tif11-17-21* has little effect on induction of *GCN4-lacZ* expression in cells expressing wild-type tRNAi in response to starvation for isoleucine and valine, which lowers TC abundance via phosphorylation of eIF2α (Fig. 5F). The ability of *tif11-17-21* to block derepression of *GCN4-lacZ* in response to the G70A substitution (Fig. 5H), but not in response to amino acid starvation (Fig. 5F), supports our proposal that G70A reduces the rate of TC binding to the PIC rather than reducing TC abundance.

Evidence that substituting G70 destabilizes the open/P_{OUT} conformation of the PIC

We sought to test our interpretation of the genetic data that G70A reduces the rate of TC binding to the PIC in a manner mitigated by the eIF1A 17-21 mutation. Measuring the rate constant for TC binding to PICs containing model mRNA(AUG) as described above revealed a dramatic ~25-fold reduction in k_{on} for TC assembled with the G70A variant of Met-tRNAi. This defect was strongly diminished in the C3U:G70A double mutant and, remarkably, was fully suppressed by the 17-21 variant of eIF1A (Fig. 6A; Table 3). The fact that the C3U substitution and eIF1A-17-21 both overcome the defect in TC binding in vitro and the Gcd⁻ phenotype in vivo conferred by G70A strongly suggests that a W:C pair at position 3:70 is required for rapid binding of TC to the open/P_{IN} conformation of the PIC (Saini et al. 2010).

Despite the ~20-fold decrease in k_{on}, the G70A substitution does not show a detectable increase in the K_d for TC in 43S·mRNA(AUG) complexes (Table 2), which

implies that it also substantially reduces the k_{off} value for these PICs. Indeed, G70A eliminates detectable dissociation of TC from 43S·mRNA(AUG) complexes, leading to nearly 100% of the complexes being in the highly stable state (Fig. 6C). G70A also significantly increases the fraction of 43S·mRNA(UUG) complexes in the highly stable state from almost none with wild type to ~70% for the mutant (Fig. 6D). These findings support the idea that, by destabilizing TC binding to the open/P_{OUT} conformation, G70A shifts the equilibrium toward the closed/P_{IN} state, which increases the probability of UUG initiation. Supporting this interpretation, combining C3U with G70A in the double mutant, which diminishes the Sui⁻ phenotype of G70A, also diminishes the increased formation of the highly stable state by 43S·mRNA(UUG) complexes conferred by G70A alone from ~70% with G70A to ~35% with C3U:G70A (Fig. 6D).

It is intriguing that the G70A substitution has little effect on the k_{on} for 43S·mRNA(UUG) complexes despite the fact that G70A reduces k_{on} for 43S·mRNA(AUG) complexes by ~20-fold (Fig. 6A,B; Table 3). If we adhere to our conclusion above that G70A decreases k_{on} for 43S·mRNA(AUG) complexes by reducing occupancy of the open/P_{OUT} state, we would expect a similar decrease for 43S·mRNA(UUG) complexes, as codons are not recognized in the open/P_{OUT} conformation. One explanation might be that the predicted reduction in k_{on} for 43S·mRNA(UUG) complexes conferred by slower TC loading to the open/P_{OUT} state is offset by an increase of nearly equal magnitude in the rate of P_{OUT}-to-P_{IN} isomerization at UUG but not AUG codons. To explain why G70A would selectively accelerate the P_{OUT}-to-P_{IN} transition at UUG, it could be proposed that G70A perturbs interaction of Met-tRNAi with eIF2 in a way that alters the orientation of TC in the P site to favor base-pairing with UUG, which entails a U:U mismatch at the first position of the codon:anticodon duplex but not for the perfect codon:anticodon duplex at AUG. We came to a similar conclusion recently regarding the *SUI5* mutation in eIF5 that stabilizes P_{IN} at UUG while destabilizing it at AUG (Martin-Marcos et al. 2014).

G31:C39 discriminates preferentially against near-cognates with first position mismatches

Results above indicate that Sui⁻ substitutions in the ASL and acceptor stem decrease initiation accuracy by distinct mechanisms. We asked whether they also differ in their effects on utilization of different near-cognates by comparing expression of firefly luciferase reporters harboring different start codons normalized for expression of a renilla luciferase reporter bearing an AUG codon (Takacs et al. 2011). Interestingly, the G31A:C39U ASL substitution elevates utilization of UUG, CUG, or GUG triplets, all first-base mismatches, but not AUA or ACG near-cognates with second- or third-base mismatches; whereas this bias does not exist for the G70A substitution in the acceptor stem (Supplemental Fig. S9). Thus, G31A:C39U differs from G70A by increasing utilization of near-cognates with first position mismatches.
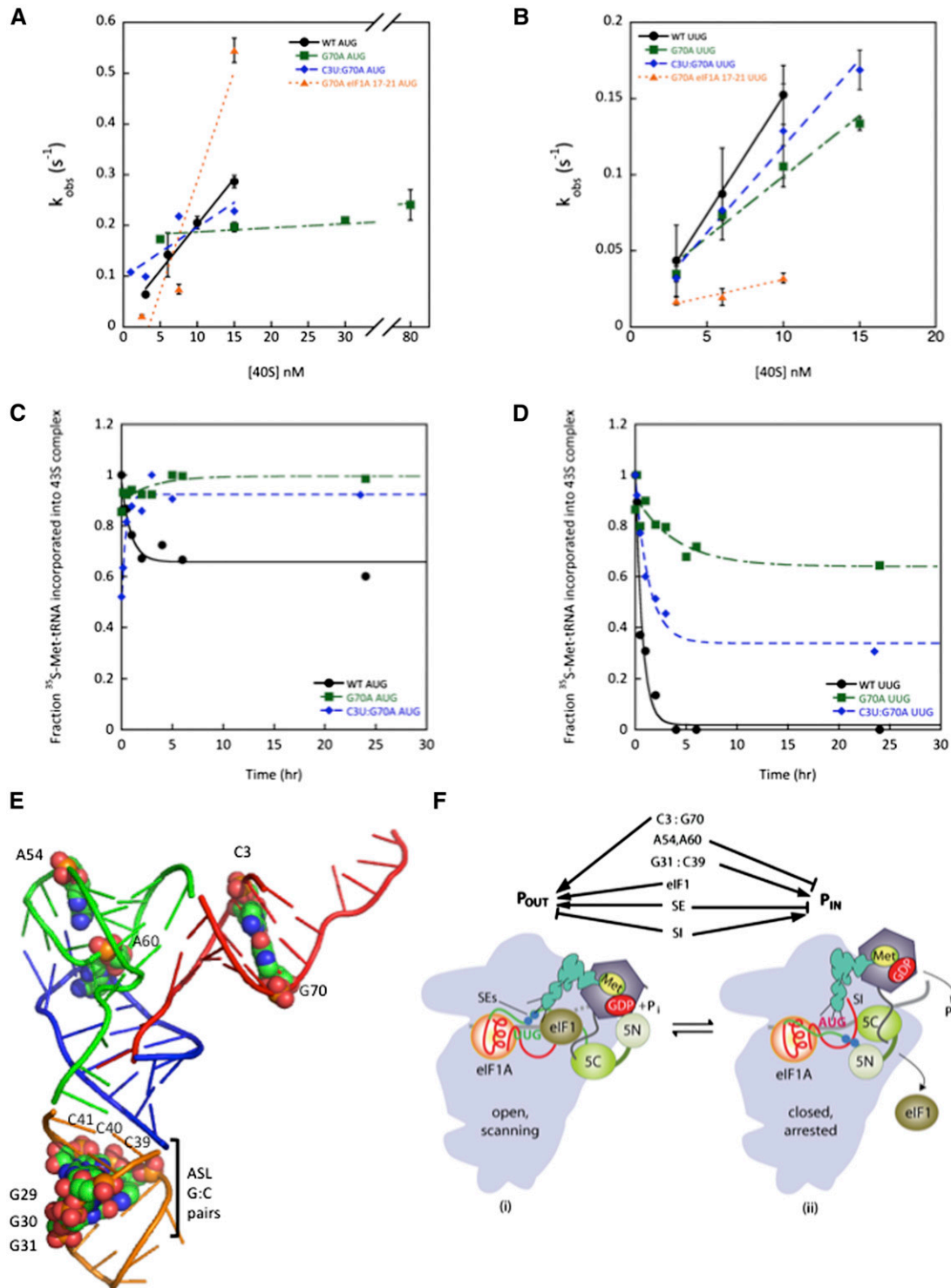
Figure 6. Disrupting acceptor stem base pair C3:G70 shifts the equilibrium from P_{OUT} to P_{IN}. (A,B) Determination of k_{on} values for TC association with 40S•eIF1•eIF1A complexes and mRNA(AUG) (A) or mRNA(UUG) (B). Each value is the average of at least two independent experiments. Errors are average deviations. (C,D) Analysis of TC dissociation from 43S·mRNA complexes for mRNA(AUG) (C) or mRNA(UUG) (D) complexes. Representative curves from at least two independent experiments are shown. k_{off} values and endpoints for dissociable complexes are given in Supplemental Table S2. (E) PyMol rendering of the crystal structure of yeast tRNA$_i$ (Protein Data Bank [PDB]: 1YFG) using color-coding to designate the acceptor stem (red), T-stem–loop (green), D-stem–loop (blue), and ASL (gold) and depicting by spheres the bases or base pairs implicated here in start codon recognition. (F) Model summarizing the deduced roles of conserved tRNA$_i$ residues in start codon recognition. See Supplemental Figure S2 for description of the open/P_{OUT} and closed/P_{IN} states of the PIC and roles of eIF1 and the SEs/SI elements of eIF1A in regulating conformational rearrangements and reactions accompanying AUG recognition. Results in this study indicate that base pair C3:G70 functions together with eIF1 and eIF1A SEs to stabilize the P_{OUT} conformation of TC binding, whereas residues A54/A60 impede rearrangement to the P_{IN} state in a manner overcome efficiently only with the perfect codon:anticodon duplex formed at AUG. G31:C39 and most likely the other two ASL G:C pairs are required for thermodynamic coupling between AUG and tRNA$_i$ in the P_{IN} state. Not summarized here is the fact that replacing G31:C39 with other Watson-Crick pairs further stabilizes P_{IN} and thereby increases initiation at NUG near-cognates (see Supplemental Figs. S11–S13 for further details.)

ASL Sui⁻ substitution G31A:C39U does not alter N6-threonylcarbamoyl modification of A37

N6-threonylcarbamoyl modification of A37 (t⁶A37) immediately adjacent to the anticodon triplet in tRNA is thought to stabilize the first base pair of the codon:anticodon duplex for the subset of tRNAs that decode ANN triplets (Agris 2008), which includes decoding of AUG by tRNA$_i$. Consistent with this, mutations that reduce t⁶A37 formation in yeast impair recognition of AUG codons (Lin et al. 2009; Daugeron et al. 2011; Srinivasan et al. 2011) and can increase the ratio of GUG to AUG initiation (El Yacoubi et al. 2011). To eliminate the possibility that G31:C39 substitutions confer Sui⁻ phenotypes by impairing t⁶A37 formation, we purified wild-type and G31A:C39U mutant tRNA$_i$, digested them with nuclease P1, and resolved the nucleoside products by high-performance liquid chromatography (HPLC). Quantification of the HPLC tracings revealed that both mutant and wild-type tRNA$_i$ contain ~1 mol of t⁶A per mole of tRNA (Supplemental Fig. S10).

Discussion

In this study, we probed the roles of highly conserved, signature residues of tRNA$_i$ in the ASL, T-loop, and acceptor stem (Fig. 6E) in determining the stability of TC binding to the PIC in vitro and the accuracy of translation initiation in vivo. Our findings implicate the ASL base pair G31:C39, T-loop residues A54,A60, and acceptor stem base pair C3:G70 in stringent AUG selection in yeast cells and indicate that these residues function by distinct biochemical mechanisms. All substitutions introducing purine:purine mismatches at any of the three G:C pairs in the ASL are lethal, as are most substitutions creating pyrimidine:pyrimidine mismatches at the first or second G:C pair. In contrast, pyrimidine:pyrimidine mismatches are tolerated at the third G:C pair, as are A:C or G:U wobble pairs at all three positions (Figs. 1F, 2F). We interpret these findings to indicate that disruption of the ASL helix is lethal and that substitutions eliminating both W:C and wobble pairing have a greater effect on helix stability for the first or second G:C pairs, owing to their internal locations, versus the third G:C pair at the end of the helix. With the exception of the G:U replacement of the third G:C pair, nonlethal substitutions introducing wobble pairs at any of these positions either have no effect on initiation accuracy or, for C41U and G31A, confer moderate hyperaccuracy (Ssu⁻) phenotypes. Much stronger Ssu⁻ phenotypes were observed for the viable replacements of the third G:C pair with the pyrimidine:pyrimidine mismatches C:C, U:C, or U:U. One way to explain these findings is to propose that any substitution that prevents both W:C and wobble pairing at any of these three positions impairs start codon recognition. For the lethal substitutions, AUG as well as near-cognate recognition would be substantially reduced, whereas nonlethal Ssu⁻ substitutions would impair AUG recognition less dramatically while still conferring a marked reduction in near-cognate (UUG) initiation.

Our biochemical analysis of the Ssu⁻ substitutions G31C and G31U, which introduce C:C or U:C mismatches at the third G:C pair, supports this view by revealing order-of-magnitude increases in K$_d$ for TC in PICs with mRNA(AUG) and an inability to form stable 43S·mRNA(UUG) complexes. In contrast, these substitutions do not reduce the affinity of TC for 43S PICs lacking mRNA, indicating that they disrupt thermodynamic coupling between Met-tRNA$_i$ and the start codon in the closed/P$_{IN}$ state. The fact that G31C and G31U evoke a more extensive reduction in the stability of the closed/P$_{IN}$ state at UUG versus AUG codons is consistent with the reduced UUG:AUG initiation ratio conferred by these Ssu⁻ mutations in vivo (Fig. 6F; Supplemental Fig. S11).

Further support for this interpretation comes from the fact that the U:U substitution of the third G:C pair, found here to confer an Ssu⁻ phenotype, was shown previously to increase the K$_d$ for TC in mRNA(AUG) complexes but not in 43S complexes lacking mRNA (Kapp et al. 2006)—the same finding made here for G31C and G31U Ssu⁻ substitutions. This defect in TC binding was fully reversed by T-loop substitutions A54U,A60C (Kapp et al. 2006), and we found here that the Ssu⁻ phenotype of the U31:U39 substitution is likewise reversed by A54U,A60C. The strong concordance between these biochemical and genetic data provides compelling evidence that the hyperaccuracy phenotypes of disrupting the third G:C pair result from a diminished contribution of base-pairing between the start codon and Met-tRNA$_i$ to the stability of the P$_{IN}$ state, which is exacerbated by the less stable codon:anticodon duplex formed at UUG triplets (Fig. 6F; Supplemental Fig. S11). It is possible that these mutations produce this effect by increasing the energetic barrier to a conformational change in the ASL that is required to attain the P$_{IN}$ state.

How might T-loop substitutions compensate for the reduced ability to access the P$_{IN}$ state at UUG codons conferred by the U31:U39 replacement? Perhaps altering the T-loop removes a structural impediment to the P$_{IN}$ state that is normally overcome by the perfect AUG:anticodon duplex (Fig. 6F). Transition to P$_{IN}$ might require deforming Met-tRNA$_i$ structure, and A54C/U substitutions would increase the flexibility of Met-tRNA$_i$ to reduce the energetic cost of this transition and increase its frequency at UUG codons. Interestingly, A54, A60, and m¹A58 in the T-loop and A20 in the D-loop participate in hydrogen bonds that rigidify the T-loop and its connection to the D-loop (Fig. 6E; Basavappa and Sigler 1991). Thus, weakening T-loop/D-loop interaction by A54 substitutions might facilitate the proposed distortion of Met-tRNA$_i$ required to achieve P$_{IN}$ in the absence of a perfect codon:anticodon match at near-cognates.

In crystal structures of bacterial 70S·mRNA·tRNA complexes, G1338 and A1339 of 16S rRNA are poised to make A-minor interactions with the minor grooves of the first and second G:C pairs in the ASL (Korostelev et al. 2006; Selmer et al. 2006), and there is evidence that these interactions stabilize Met-tRNA$_i$ binding to the 70S P site (Lancaster and Noller 2005; Qin et al. 2007). Our finding that purine:purine and most pyrimidine:pyrimidine

mismatches are not tolerated at the first and second G:C pairs is consistent with this mechanism operating in yeast. This model can also explain our previous results indicating that nearly all substitutions of the corresponding yeast 18S rRNA residues (G1575 and A1576) are lethal and impair AUG recognition in cells coexpressing wild-type rRNA (Dong et al. 2008). The lethal or Ssu⁻ phenotypes of substitutions disrupting W:C pairing at the third G:C pair might also be attributed to an indirect disruption of A-minor interactions made by the adjacent G:C pairs. Our finding that W:C substitutions at 29:41 or 30:40 have little effect on cell growth is not inconsistent with the model because, with few exceptions, the stabilities of A-minor interactions vary little with different W:C pairs as receptors (Doherty et al. 2001; Battle and Doudna 2002). Harder to explain, however, is the absence of strong phenotypes associated with various substitutions that introduce wobble pairs at 29:41 or 30:40, which should strongly destabilize A-minor interactions (Battle and Doudna 2002). Therefore, more work is required to determine whether A-minor interactions of G1575 and A1576 with the ASL G:C pairs play a critical role in stabilizing the P_{IN} conformation and account for the lethal or hyperaccuracy phenotypes of disrupting the ASL G:C base pairs.

In contrast to the Ssu⁻ phenotypes produced by mutations that eliminate base-pairing in the ASL, it is striking that replacing the third G:C pair with any other W:C pair reduces accuracy and confers a marked Sui⁻ phenotype. Our biochemical analysis of Sui⁻ substitutions G31C:C39G and G31U:C39A showed that they increase the stability of TC binding with AUG and UUG codons in the P site to the point where dissociation of TC from the PICs was undetectable. Because TC formed with wild-type Met-tRNA$_i$ dissociates more rapidly from UUG than from AUG complexes, the stabilization of PICs conferred by these substitutions appears to be relatively greater at UUG codons, consistent with their Sui⁻ phenotypes. Interestingly, the G31A:C39U replacement specifically increased utilization of near-cognates with first position mismatches (CUG and GUG in addition to UUG) but not second or third position mismatches (AUA and ACG). Thus, while a base pair per se is required at position 31:39 for thermodynamic coupling between the start codon and anticodon of tRNA$_i$, a G:C pair is needed specifically to enforce a requirement for an A:U pair at the first position of the codon:anticodon helix.

One way to explain our finding that W:C replacements of G31:C39 stabilize P_{IN} at AUG or UUG codons is to propose that, compared with other Watson-Crick base pairs, the wild-type G31:C39 base pair imposes an impediment to P_{IN} that can be overcome efficiently only with the perfect codon:anticodon duplex formed at AUG codons. In this view, W:C replacements at 31:39 reduce this impediment, allowing "NUG" near-cognates to overcome the impediment more effectively. We envision that G31:C39, being the last base pair of the ASL, promotes a rigid conformation of the anticodon loop that clashes with a P-site element, and this clash is eliminated by a conformational change triggered by the first base pair of the codon:anticodon duplex. G31:C39 would be optimized

to impart this inhibitory conformation of the anticodon loop in a way that could not be replaced by other W:C pairs at this position. The fact that W:C replacements at the first or second G:C pairs evoke considerably weaker Sui⁻ phenotypes could be explained by proposing that they act indirectly to diminish the critical function of G31:C39 in blocking the transition to P_{IN} at NUG near-cognates (Supplemental Fig. S12). Interestingly, the ASL in the crystal structure of *Escherichia coli* tRNA$_i$ displays a noncanonical conformation in which A37 interacts with G29:C41 instead of stacking on residue 36 of the anticodon loop, the ASL helix is extended by a C32:A38 base pair, and its major groove is obscured (Barraud et al. 2008). If this noncanonical conformation occurs in yeast tRNA$_i$, it might be stabilized by G31:C39, and an A:U base pair at the first position of the codon:anticodon duplex could be required for isomerization to the conformation needed for a stable P_{IN} state.

There is evidence that the G1338A substitution of 16S rRNA, which appears to enhance its A-minor interaction with the ASL of tRNA$_i$, decreases initiation fidelity by compensating for mismatches in the start codon:anticodon helix (Qin et al. 2007). It is unlikely that this phenomenon is involved in the moderate Sui⁻ phenotypes of W:C replacements at G29:C41 and G30:C40 because these W:C replacements should, if anything, decrease the stability of A-minor interactions and increase accuracy by discriminating against mismatched codon:anticodon duplexes. Hence, we favor the alternative explanation that the W:C replacements at G29:C41 and G30:C40 decrease accuracy indirectly by impairing the critical function of G31:C39 in discriminating against near-cognates.

Although the C3:G70 base pair in the acceptor stem is a highly conserved feature of tRNA$_i$ (Marck and Grosjean 2002), no function had been ascribed to it. We found that mutations disrupting W:C pairing at C3:G70 decrease accuracy but, unlike Sui⁻ substitutions of G31:C39, also confer the Gcd⁻ phenotype signifying slower TC loading to the open conformation of the PIC. Importantly, the Sui⁻ and Gcd⁻ phenotypes of G70 substitutions were cosuppressed by the 17-21 substitution in the eIF1A NTT. The *17-21* mutation was shown previously to stabilize the open/P_{OUT} conformation of the PIC (Fekete et al. 2007; Saini et al. 2010) and cosuppress Gcd⁻ and Sui⁻ phenotypes conferred by mutations inactivating the SEs in the eIF1A CTT (Supplemental Fig. S2; Saini et al. 2010) and by other mutations eliminating 40S contact sites in eIF1 (Martin-Marcos et al. 2013). Hence, an attractive model is that C3:G70 in tRNA$_i$ acts together with eIF1 and the eIF1A SEs to promote TC binding in the P_{OUT} conformation. Disrupting C3:G70 would destabilize P_{OUT}, reducing the rate of TC loading (for the Gcd⁻ phenotype), and allow more frequent rearrangement to the P_{IN} conformation at UUG codons (for the Sui⁻ phenotype) (Fig. 6F; Supplemental Fig. S13).

Strong support for this model comes from our in vitro findings that G70A greatly reduces the k_{on} for TC binding to 43S·mRNA(AUG) complexes in a manner mitigated by the C3U substitution (which restores W–C pairing) and fully suppressed by eIF1A-17-21. Because 17-21 stabilizes the open/P_{OUT} conformation (Cheung et al. 2007; Fekete

et al. 2007; Saini et al. 2010), its ability to suppress the k_{on} defect of G70A supports the idea that G70A decreases the rate of TC binding specifically to the P_{OUT} conformation. Consistent with this, G70A stabilizes the P_{IN} state, as it reduces the rate of TC dissociation from PICs reconstituted with mRNA(AUG) or mRNA(UUG), and this defect for mRNA(UUG) complexes was diminished by C3U. This last finding supports the idea that by disrupting C3:G70, G70A elevates UUG initiation by stabilizing P_{IN} at UUG codons. Because G70A has a much smaller effect on the k_{on} of TC in PICs reconstituted with mRNA(UUG) versus mRNA(AUG), we inferred that it also increases the rate of P_{OUT}-to-P_{IN} isomerization specifically at UUG codons, which should contribute to its Sui$^-$ phenotype (Supplemental Fig. S13).

One way to explain the ability of G70A to disfavor the P_{OUT} mode of TC binding is to propose that eliminating the C3:G70 pair destabilizes the acceptor stem and renders the connection between Met-tRNA$_i$ and eIF2 more flexible in a manner that is particularly detrimental for binding in the P_{OUT} state. The recent crystal structure of a *Tetrahymena* 40S·eIF1·eIF1A complex reveals that the SI element of the eIF1A NTT bridges a connection between the head and body of the 40S subunit (Weisser et al. 2013), which might indicate that the 17-21 substitution in the NTT shifts the equilibrium from P_{IN} to P_{OUT} and thereby restores rapid TC loading by the G70A variant by weakening this connection within the 40S subunit. However, why this enhancement occurs at AUG but not UUG codons is not yet clear.

In summary, our results provide compelling evidence that the distinctive C3:G70 base pair in the acceptor stem is important for rapid TC binding in the P_{OUT} conformation of the PIC and functions with eIF1 and the eIF1A SEs to discriminate against UUG start codons by impeding the P_{OUT}-to-P_{IN} transition at near-cognate triplets. In contrast, G31:C39 in the ASL and A54 in the T-loop appear to function differently to block UUG initiation by imposing an impediment to P_{IN} that can be overcome only with a perfect AUG:anticodon duplex, with G31:C39 specifically enforcing the requirement for an A:U pair at the first position of the AUG:anticodon duplex. While G31:C39 discriminates against NUG near-cognates, a Watson-Crick base pair is required at this position in the ASL for P_{IN} stability and efficient start codon recognition, and disrupting base pairing at this position discriminates against near-cognates. Thus, different regions of tRNA$_i$ perform distinct functions in the PIC to promote AUG recognition in vivo. Considering that the signature residues of tRNA$_i$ are conserved in all kingdoms of life, the functions ascribed here to these residues of yeast tRNA$_i$ likely apply to tRNA$_i$ in mammals and other eukaryotes.

Materials and methods

Plasmids and yeast strains

Plasmids and yeast strains are listed in Supplemental Tables S3 and S5, respectively, and details of their construction are provided in the Supplemental Material.

Biochemical analyses of yeast cells

Northern analyses of tRNA$_i$ expression were conducted as described previously (Anderson et al. 1998). tRNA aminoacylation in vivo was analyzed using RNA isolated (Zaborske et al. 2009) and subjected to Northern analysis (Varshney et al. 1991) as previously described using oligonucleotide probes listed in the Supplemental Material. Assays of β-galactosidase activity in whole-cell extracts were performed as described previously (Moehle and Hinnebusch 1991), as were measurements of luminescence in whole-cell extracts (Dyer et al. 2000). Coimmunoprecipitation analysis of the TC was performed as described previously (Dev et al. 2010) using antibodies against Flag (Sigma) and Gcd11 (provided by E. Hannig).

Biochemical analysis in the reconstituted yeast translation system

Purification of 40S ribosomal subunits and eIF1, eIF1A, and eIF2 as well as preparation of mRNA and tRNA$_i$ variants charged with [^{35}S]-labeled or unlabeled methionine were performed as described (Acker et al. 2007). A double filter-binding assay was used to measure K_d values of [^{35}S]-Met-tRNA$_i$ variants and eIF2-GDPNP essentially as described previously (Acker et al. 2007). The K_d values of TC (assembled with [^{35}S]-Met-tRNA$_i$ variants) and 40S·eIF1·eIF1A·mRNA PICs and the rate constants of TC association/dissociation for the same PICs were determined by gel shift assays as described previously (Kolitz et al. 2009) with slight modifications described in the Supplemental Material.

References

Acker MG, Kolitz SE, Mitchell SF, Nanda JS, Lorsch JR. 2007. Reconstitution of yeast translation initiation. *Methods Enzymol* **430:** 111–145.

Agris PF. 2008. Bringing order to translation: The contributions of transfer RNA anticodon-domain modifications. *EMBO Rep* **9:** 629–635.

Algire MA, Maag D, Lorsch JR. 2005. Pi release from eIF2, not GTP hydrolysis, is the step controlled by start-site selection during eukaryotic translation initiation. *Mol Cell* **20:** 251–262.

Alone PV, Cao C, Dever TE. 2008. Translation initiation factor 2γ mutant alters start codon selection independent of Met-tRNA binding. *Mol Cell Biol* **28:** 6877–6888.

Anderson J, Phan L, Cuesta R, Carlson BA, Pak M, Asano K, Bjork GR, Tamame M, Hinnebusch AG. 1998. The essential Gcd10p–Gcd14p nuclear complex is required for 1-methyladenosine modification and maturation of initiator methionyl-tRNA. *Genes Dev* **12:** 3650–3662.

Astrom SU, von Pawel-Rammingen U, Bystrom AS. 1993. The yeast initiator tRNA^{Met} can act as an elongator tRNA^{Met} in vivo. *J Mol Biol* **233:** 43–58.

Barraud P, Schmitt E, Mechulam Y, Dardel F, Tisne C. 2008. A unique conformation of the anticodon stem–loop is associated with the capacity of tRNAfMet to initiate protein synthesis. *Nucleic Acids Res* **36:** 4894–4901.

Basavappa R, Sigler PB. 1991. The 3 Å crystal structure of yeast initiator tRNA: Functional implications in initiator/elongator discrimination. *EMBO J* **10:** 3105–3111.

Battle DJ, Doudna JA. 2002. Specificity of RNA-RNA helix recognition. *Proc Natl Acad Sci* **99:** 11676–11681.

Boeke JD, Trueheart J, Natsoulis G, Fink GR. 1987. 5-fluoro-orotic acid as a selective agent in yeast molecular genetics. *Methods Enzymol* **154:** 164–175.

Cheung YN, Maag D, Mitchell SF, Fekete CA, Algire MA, Takacs JE, Shirokikh N, Pestova T, Lorsch JR, Hinnebusch AG. 2007. Dissociation of eIF1 from the 40S ribosomal subunit is a key step in start codon selection in vivo. *Genes Dev* **21:** 1217–1230.

Daugeron MC, Lenstra TL, Frizzarin M, El Yacoubi B, Liu X, Baudin-Baillieu A, Lijnzaad P, Decourty L, Saveanu C, Jacquier A, et al. 2011. Gcn4 misregulation reveals a direct role for the evolutionary conserved EKC/KEOPS in the t6A modification of tRNAs. *Nucleic Acids Res* **39:** 6148–6160.

Dev K, Qiu H, Dong J, Zhang F, Barthlme D, Hinnebusch AG. 2010. The β/Gcd7 subunit of eukaryotic translation initiation factor 2B (eIF2B), a guanine nucleotide exchange factor, is crucial for binding eIF2 in vivo. *Mol Cell Biol* **30:** 5218–5233.

Dever TE, Yang W, Åström S, Byström AS, Hinnebusch AG. 1995. Modulation of tRNA$_i^{Met}$, eIF-2 and eIF-2B expression shows that *GCN4* translation is inversely coupled to the level of eIF-2·GTP·Met-tRNA$_i^{Met}$ ternary complexes. *Mol Cell Biol* **15:** 6351–6363.

Doherty EA, Batey RT, Masquida B, Doudna JA. 2001. A universal mode of helix packing in RNA. *Nat Struct Biol* **8:** 339–343.

Donahue T. 2000. Genetic approaches to translation initiation in *Saccharomyces cerevisiae*. In *Translational control of gene expression* (ed. N Sonenberg, et al.), pp. 487–502. Cold Spring Harbor Laboratory Press, Cold Spring Harbor, NY.

Dong J, Nanda JS, Rahman H, Pruitt MR, Shin BS, Wong CM, Lorsch JR, Hinnebusch AG. 2008. Genetic identification of yeast 18S rRNA residues required for efficient recruitment of initiator tRNA(Met) and AUG selection. *Genes Dev* **22:** 2242–2255.

Drabkin HJ, Helk B, RajBhandary UL. 1993. The role of nucleotides conserved in eukaryotic initiator methionine tRNAs in initiation of protein synthesis. *J Biol Chem* **268:** 25221–25228.

Dyer BW, Ferrer FA, Klinedinst DK, Rodriguez R. 2000. A noncommercial dual luciferase enzyme assay system for reporter gene analysis. *Anal Biochem* **282:** 158–161.

El Yacoubi B, Hatin I, Deutsch C, Kahveci T, Rousset JP, Iwata-Reuyl D, Murzin AG, de Crecy-Lagard V. 2011. A role for the universal Kae1/Qri7/YgjD (COG0533) family in tRNA modification. *EMBO J* **30:** 882–893.

Farruggio D, Chaudhuri J, Maitra U, RajBhandary UL. 1996. The A1 U72 base pair conserved in eukaryotic initiator tRNAs is important specifically for binding to the eukaryotic translation initiation factor eIF2. *Mol Cell Biol* **16:** 4248–4256.

Fekete CA, Mitchell SF, Cherkasova VA, Applefield D, Algire MA, Maag D, Saini A, Lorsch JR, Hinnebusch AG. 2007. N-and C-terminal residues of eIF1A have opposing effects on the fidelity of start codon selection. *EMBO J* **26:** 1602–1614.

Hashem Y, des Georges A, Dhote V, Langlois R, Liao HY, Grassucci RA, Hellen CU, Pestova TV, Frank J. 2013. Structure of the mammalian ribosomal 43S preinitiation complex bound to the scanning factor DHX29. *Cell* **153:** 1108–1119.

Hinnebusch AG. 2005. Translational regulation of GCN4 and the general amino acid control of yeast. *Annu Rev Microbiol* **59:** 407–450.

Hinnebusch AG. 2011. Molecular mechanism of scanning and start codon selection in eukaryotes. *Microbiol Mol Biol Rev* **75:** 434–467.

Kapp LD, Lorsch JR. 2004. GTP-dependent recognition of the methionine moiety on initiator tRNA by translation factor eIF2. *J Mol Biol* **335:** 923–936.

Kapp LD, Kolitz SE, Lorsch JR. 2006. Yeast initiator tRNA identity elements cooperate to influence multiple steps of translation initiation. *RNA* **12:** 751–764.

Kolitz SE, Takacs JE, Lorsch JR. 2009. Kinetic and thermodynamic analysis of the role of start codon/anticodon base pairing during eukaryotic translation initiation. *RNA* **15:** 138–152.

Korostelev A, Trakhanov S, Laurberg M, Noller HF. 2006. Crystal structure of a 70S ribosome-tRNA complex reveals functional interactions and rearrangements. *Cell* **126:** 1065–1077.

Lancaster L, Noller HF. 2005. Involvement of 16S rRNA nucleotides G1338 and A1339 in discrimination of initiator tRNA. *Mol Cell* **20:** 623–632.

Lin CA, Ellis SR, True HL. 2009. The Sua5 protein is essential for normal translational regulation in yeast. *Mol Cell Biol* **30:** 354–363.

Lomakin IB, Steitz TA. 2013. The initiation of mammalian protein synthesis and mRNA scanning mechanism. *Nature* **500:** 307–311.

Lomakin IB, Shirokikh NE, Yusupov MM, Hellen CU, Pestova TV. 2006. The fidelity of translation initiation: Reciprocal activities of eIF1, IF3 and YciH. *EMBO J* **25:** 196–210.

Maag D, Fekete CA, Gryczynski Z, Lorsch JR. 2005. A conformational change in the eukaryotic translation preinitiation complex and release of eIF1 signal recognition of the start codon. *Mol Cell* **17:** 265–275.

Mandal N, Mangroo D, Dalluge JJ, McCloskey JA, Rajbhandary UL. 1996. Role of the three consecutive G:C base pairs conserved in the anticodon stem of initiator tRNAs in initiation of protein synthesis in *Escherichia coli*. *RNA* **2:** 473–482.

Marck C, Grosjean H. 2002. tRNomics: Analysis of tRNA genes from 50 genomes of Eukarya, Archaea, and Bacteria reveals anticodon-sparing strategies and domain-specific features. *RNA* **8:** 1189–1232.

Martin-Marcos P, Nanda J, Luna RE, Wagner G, Lorsch JR, Hinnebusch AG. 2013. β-Hairpin loop of eIF1 mediates 40S ribosome binding to regulate initiator tRNAMet recruitment and accuracy of AUG selection in vivo. *J Biol Chem* **38:** 27546–27562.

Martin-Marcos P, Nanda JS, Luna RE, Zhang F, Saini AK, Cherkasova VA, Wagner G, Lorsch JR, Hinnebusch AG. 2014. Enhanced eIF1 binding to the 40S ribosome impedes conformational rearrangements of the preinitiation complex and elevates initiation accuracy. *RNA* **20:** 150–167.

Moehle CM, Hinnebusch AG. 1991. Association of RAP1 binding sites with stringent control of ribosomal protein gene transcription in *Saccharomyces cerevisiae*. *Mol Cell Biol* **11:** 2723–2735.

Nanda JS, Saini AK, Munoz AM, Hinnebusch AG, Lorsch JR. 2013. Coordinated movements of eukaryotic translation initiation factors eIF1, eIF1A, and eIF5 trigger phosphate release from eIF2 in response to start codon recognition by the ribosomal preinitiation complex. *J Biol Chem* **288:** 5316–5329.

Passmore LA, Schmeing TM, Maag D, Applefield DJ, Acker MG, Algire MA, Lorsch JR, Ramakrishnan V. 2007. The eukaryotic translation initiation factors eIF1 and eIF1A induce an open conformation of the 40S ribosome. *Mol Cell* **26:** 41–50.

Pestova TV, Lorsch JR, Hellen CUT. 2007. The mechanism of translation initiation in eukaryotes. In *Translational control in biology and medicine* (ed. M Mathews, et al.), pp. 87–128. Cold Spring Harbor Laboratory Press, Cold Spring Harbor, NY.

Qin D, Abdi NM, Fredrick K. 2007. Characterization of 16S rRNA mutations that decrease the fidelity of translation initiation. *RNA* **13:** 2348–2355.

Rabl J, Leibundgut M, Ataide SF, Haag A, Ban N. 2011. Crystal structure of the eukaryotic 40S ribosomal subunit in complex with initiation factor 1. *Science* **331:** 730–736.

RajBhandary UL. Chow CM. 1995. Initiator tRNAs and initiation of protein synthesis. In *tRNA structure, biosynthesis, and function* (ed. D Soll and UL RajBhandary), pp. 511–528. American Society for Microbiology Press, Washington, DC.

Saini AK, Nanda JS, Lorsch JR, Hinnebusch AG. 2010. Regulatory elements in eIF1A control the fidelity of start codon selection by modulating tRNA(i)(Met) binding to the ribosome. *Genes Dev* **24:** 97–110.

Selmer M, Dunham CM, Murphy FV IV, Weixlbaumer A, Petry S, Kelley AC, Weir JR, Ramakrishnan V. 2006. Structure of the 70S ribosome complexed with mRNA and tRNA. *Science* **313:** 1935–1942.

Shin BS, Kim JR, Walker SE, Dong J, Lorsch JR, Dever TE. 2011. Initiation factor eIF2 promotes eIF2-GTP-Met-tRNA(i)(Met) ternary complex binding to the 40S ribosome. *Nat Struct Mol Biol* **18:** 1227–1234.

Srinivasan M, Mehta P, Yu Y, Prugar E, Koonin EV, Karzai AW, Sternglanz R. 2011. The highly conserved KEOPS/EKC complex is essential for a universal tRNA modification, t6A. *EMBO J* **30:** 873–881.

Takacs JE, Neary TB, Ingolia NT, Saini AK, Martin-Marcos P, Pelletier J, Hinnebusch AG, Lorsch JR. 2011. Identification of compounds that decrease the fidelity of start codon recognition by the eukaryotic translational machinery. *RNA* **17:** 439–452.

Valasek L, Nielsen KH, Zhang F, Fekete CA, Hinnebusch AG. 2004. Interactions of eukaryotic translation initiation factor 3 (eIF3) subunit NIP1/c with eIF1 and eIF5 promote preinitiation complex assembly and regulate start codon selection. *Mol Cell Biol* **24:** 9437–9455.

Varshney U, Lee CP, RajBhandary UL. 1991. Direct analysis of aminoacylation levels of tRNA as in vivo. *J Biol Chem* **266:** 24712–24718.

Varshney U, Lee CP, RajBhandary UL. 1993. From elongator tRNA to initiator tRNA. *Proc Natl Acad Sci* **90:** 2305–2309.

von Pawel-Rammingen U, Astrom S, Bystrom AS. 1992a. Mutational analysis of conserved positions potentially important for initiator tRNA function in *Saccharomyces cerevisiae*. *Mol Cell Biol* **12:** 1432–1442.

Weisser M, Voigts-Hoffmann F, Rabl J, Leibundgut M, Ban N. 2013. The crystal structure of the eukaryotic 40S ribosomal subunit in complex with eIF1 and eIF1A. *Nat Struct Mol Biol* **20:** 1015–1017.

Yoon HJ, Donahue TF. 1992. The *sui1* suppressor locus in *Saccharomyces cerevisiae* encodes a translation factor that functions during $tRNA_i^{Met}$ recognition of the start codon. *Mol Cell Biol* **12:** 248–260.

Yu Y, Marintchev A, Kolupaeva VG, Unbehaun A, Veryasova T, Lai SC, Hong P, Wagner G, Hellen CU, Pestova TV. 2009. Position of eukaryotic translation initiation factor eIF1A on the 40S ribosomal subunit mapped by directed hydroxyl radical probing. *Nucleic Acids Res* **37:** 5167–5182.

Zaborske JM, Narasimhan J, Jiang L, Wek SA, Dittmar KA, Freimoser F, Pan T, Wek RC. 2009. Genome-wide analysis of tRNA charging and activation of the eIF2 kinase Gcn2p. *J Biol Chem* **284:** 25254–25267.